

CLEARINGHOUSE FOR FEDERAL SCIENTIFIC AND TECHNICAL INFORMATION CFSTI
DOCUMENT MANAGEMENT BRANCH 410.11

LIMITATIONS IN REPRODUCTION QUALITY

ACCESSION =

Handwritten: H-60-112

- ☒ 1. WE REGRET THAT LEGIBILITY OF THIS DOCUMENT IS IN PART UNSATISFACTORY. REPRODUCTION HAS BEEN MADE FROM BEST AVAILABLE COPY.
- ☒ 2. A PORTION OF THE ORIGINAL DOCUMENT CONTAINS FINE DETAIL WHICH MAY MAKE READING OF PHOTOCOPY DIFFICULT.
- ☐ 3. THE ORIGINAL DOCUMENT CONTAINS COLOR, BUT DISTRIBUTION COPIES ARE AVAILABLE IN BLACK-AND-WHITE REPRODUCTION ONLY.
- ☐ 4. THE INITIAL DISTRIBUTION COPIES CONTAIN COLOR WHICH WILL BE SHOWN IN BLACK-AND-WHITE WHEN IT IS NECESSARY TO REPRINT.
- ☐ 5. LIMITED SUPPLY ON HAND: WHEN EXHAUSTED, DOCUMENT WILL BE AVAILABLE IN MICROFICHE ONLY.
- ☐ 6. LIMITED SUPPLY ON HAND: WHEN EXHAUSTED DOCUMENT WILL NOT BE AVAILABLE.
- ☐ 7. DOCUMENT IS AVAILABLE IN MICROFICHE ONLY.
- ☐ 8. DOCUMENT AVAILABLE ON LOAN FROM CFSTI (TT DOCUMENTS ONLY).
- ☐ 9.

FINAL PROGRESS REPORT

1 January 1962 to 1 May 1964

HIGH POWER SEMICONDUCTOR

PHASE SHIFTING DEVICES

Contract NObsr - 87291

Project Serial No. SR 008-03-02

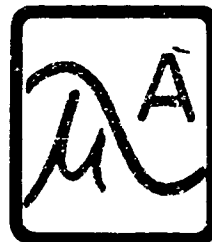
Task 9637

Navy Department, Bureau of Ships

Electronics Division

93-j-8.60
~~2.25~~

MICROWAVE
ASSOCIATES,
INC.



FINAL PROGRESS REPORT

1 JANUARY 1962 to 1 May 1964

HIGH POWER SEMICONDUCTOR PHASE SHIFTING DEVICES

Contract NObsr-87291

Project Serial No. SR 008-03-02, Task 9637

Navy Department, Bureau of Ships, Electronics Division

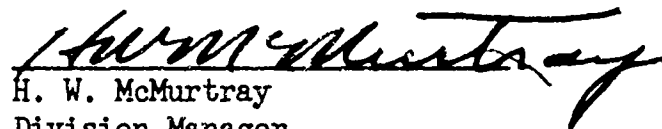
This contract constitutes a direct extension of the work done on Contract NObsr-81470, entitled "Phase Shifter Study (Non-Ferrite)", which terminated with the Sixth Quarterly Progress Report.

Prepared by:



Joseph F. White
Project Manager

Approved by:



H. W. McMurtray
Division Manager
Solid-State Circuits Division

May, 1964

MICROWAVE ASSOCIATES, INC.
BURLINGTON, MASSACHUSETTS

TABLE OF CONTENTS

	<u>Page No.</u>
I	
A. Table of Contents	I-1
B. List of Illustrations	I-4
C. Abstract	I-7
D. Purpose	I-8
E. Identification of Personnel	I-9
II	
Introduction	II-1
A. High Power Phase Shifting	II-1
B. Low Power Phase Shifting	II-3
III	
The Transmission Reflection Mode	III-1
A. Circuit Configuration	III-1
1. Matched Transmission Requirements	III-2
2. Controlled Reflection Terminations	III-5
a) Continuous	III-5
b) Step	III-5
B. Circuit Implementation	III-10
1. Continuous Type	III-10
a) Analytical Procedure	III-10
b) L-Band Model	III-10
c) S-Band Model	III-16
d) RF Power Limit	III-19
e) Temperature Effects	III-21

TABLE OF CONTENTS

(con't.)

Page No.

III	B.	2. Step Type	III-21
		a) General Comments	III-21
		b) L-Band Model	III-24
		c) S-Band Model	III-29
		d) RF Power Limits	III-33
IV		The Transmission Mode	IV-1
	A.	Design Considerations	IV-1
		1. Introductory Remarks	IV-1
		2. Phase Shift and Transmission Match	IV-1
		a) Equivalent Line	IV-1
		b) Maximum VSWR	IV-1
		c) Phase Shift Approximation	IV-4
		d) Exact Solution for Cascade Circuit	IV-6
		e) Approximate Loss Expressions	IV-6
	B.	Circuit Implementation	IV-9
		1. L-Band Circuit	IV-9
		a) Stub Approach	IV-9
		b) Measured Characteristics	IV-11
		c) Peak Power Limits	IV-15
		d) Variation of Phase Shift with Frequency	IV-18

TABLE OF CONTENTS

(con't.)

Page No.

IV	B	2. S-Band Circuit	IV-20
		a) LC Circuit Approach	IV-20
		b) Variation of Phase Shift with Frequency	IV-28
		c) Measured Characteristics	IV-28
		d) Peak Power Limits	IV-36
V		Conclusions	V-1
VI		Bibliography	VI-1

Distribution List

I B.

LIST OF ILLUSTRATIONS

<u>FIGURE</u>	<u>SECTION</u>	<u>CAPTION</u>
1	III-A-1	Transmission-Reflection Phase Shifters
2	III-A-1	Reflectively Terminated Hybrid Coupler Equations
3	III-A-1	Theoretical VSWR _{in} versus Frequency Characteristic of a Reflectively Terminated Hybrid Coupler
4	III-A-1	Measured and Calculated VSWR _{in} of Symmetric Open Circuit Terminated Hybrid Coupler
5	III-A-2	Controlled Reflection Terminations
6	III-A-2	Continuously Phase Variable Single Varactor Termination
7	III-A-2	Continuously Phase Variable, Two Varactor Termination
8	III-B-1-a	Varactor Termination Parameters
9	III-B-1-a	Varactor Termination Admittance Plot
10	III-B-1-b	Measured and Calculated Values of Continuous Phase Shift
11	III-B-1-b	Measured Values of Phase Shifter Insertion Loss
12	III-B-1-b	Phase Shift and Insertion Loss of L-Band Phase Shifter
13	III-B-1-c	Phase Shift and Insertion Loss of S-Band Phase Shifter
14	III-B-1-d	Effect of Increasing RF Power in a Continuous Phase Shifter
15	III-B-1-e	Phase Shift versus Bias with Temperature as Parameter
16	III-B-2-a	The Transmission Reflection Phase Shifter
17	III-B-2-a	Phase Shift versus Peak Power

LIST OF ILLUSTRATIONS

(con't.)

<u>FIGURE</u>	<u>SECTION</u>	<u>CAPTION</u>
18	III-B-2-a	4-Bit Phase Shift versus Bias
19	III-B-2-a	Insertion Loss and VSWR
20	III-B-2-c	S-Band Step Phase Shifter Equivalent Circuit
21	III-B-2-c	Step Phase Shifter Phase Shift
22	III-B-2-c	Step Phase Shifter Insertion Loss
23	IV-A-1 & IV-A-2-c	Transmission Phase Shifter
24	IV-A-1	Geometric Description of Phase Shift Approximation
25	IV-A-2-a	Equivalent Line Length Approximation
26	IV-A-2-d	Exact Gain Expression for Transmission Phase Shifter Cascade
27	IV-B-1-a	L-Band Transmission Phase Shifter Prototype
28	IV-B-1-b	Photograph of L-Band Transmission Phase Shifter
29	IV-B-1-b	Measured Phase Shift of L-Band Model
30	IV-B-1-b	Measured Insertion Loss of L-Band Model
31	IV-B-1-c	Phase Shift versus Peak Power Obtained with Transmission Circuit Using Two 800 Volt Switching Diodes
32	IV-B-1-d	Calculated and Measured Phase Shift versus Frequency
33	IV-B-2-a	PIN Diode Equivalent Circuit
34	IV-B-2-a IV-B-2-d	Equivalent Circuit, with Loss, of Iteratively Loaded Line Phase Shifter Prototype Network
35	IV-B-2-b	Susceptance versus Frequency Diagram

LIST OF ILLUSTRATIONS

(con't.)

<u>FIGURE</u>	<u>SECTION</u>	<u>CAPTION</u>
36	IV-B-2-c	Photograph of Two Section Transmission Phase Shifter
37	IV-B-2-c	Phase Shift Characteristic of Two Section Phase Shifter
38	IV-B-2-b	Insertion Loss Characteristic of Two Section Transmission Phase Shifter
39	IV-B-2-b	VSWR Characteristic of Two Section Transmission Phase Shifter
40	IV-B-2-b	Photograph of S-Band Transmission Phase Shifter
41	IV-B-2-b	Performance of S-Band, 8 Section Iterative Phase Shifter with Diodes Removed
42	IV-B-2-b	S-Band Transmission Phase Shifter Performance

I C. ABSTRACT

~~This~~ report summarizes the efforts ~~by Microwave Associates~~ to investigate semiconductor phase shifting techniques in the L and S frequency bands. The summary describes analyses and experimental studies of two basic phase shifter circuit modes, the transmission phase shifter and the transmission-reflection phase shifter. In the latter class, both continuous and discrete increment phase control models are treated.

Highest power and lowest insertion loss results were obtained using the transmission mode enhancing its usefulness in phased array radar. ~~This PIN diode phase shifter provided peak power operation at 15 kilowatts at both L and S bands with total insertion loss values 0.7 and 0.9 decibels respectively for 180°, 8 equal increment phase shift characteristics. Peak power operation to 37 kilowatts at S-band and 140 kilowatts at L-band were realized with smaller phase shift values.~~

The transmission reflection circuit mode utilizing PIN diodes for phase control basically yields switchable time delay, and models were constructed which were operated to 48 kilowatts at L-band and 5 kilowatts at S-band.

Continuous phase control for low power applications was demonstrated at L and S-bands with a figure of merit of approximately 250 degrees phase shift per decibel of insertion loss per kilo-megacycle of operation using the transmission reflection mode. These used 180 Kmc cut-off frequency varactors as phase control elements. () ↗

I D. PURPOSE

The purpose of this work is to investigate microwave phase shifting techniques, excluding ferromagnetic and mechanical methods, to make recommendations for new phase shifting techniques which provide improved electronic control, and to develop phase shifter models utilizing these techniques.

I E. IDENTIFICATION OF PERSONNEL

<u>Name</u>	<u>Title</u>
J. White	Project Manager
L. Mesler	Semiconductor Engineer
R. Galvin	Diode Characterization Engineer
H. Griffin	Circuit Engineer
Dr. K. Mortenson	Consulting Physicist

Biographies of these personnel have been included in the previous reports.

II INTRODUCTION

A. High Power Phase Shifting

The desirability of radar systems having large RF power capability as well as rapid antenna pointing agility suggests the use of phased array antenna techniques. Such phased array antennas require precise RF phase control, and for this function various schemes have been recommended and tried within the last few years.

These methods have included phase control at IF frequencies and the deployment of frequency multiplying chains to obtain microwave energy of controlled phase. Another technique consists of the use of sections of waveguide with spaced apertures through which microwave energy may escape by radiation; the direction of radiation may be controlled by adjustment of the frequency of the microwave energy; this technique makes use of the dispersive property of waveguide when operated in a transmission mode near cut-off. Using this technique, beam steering can be accomplished at a rate that is limited only by that rate at which the transmission frequency can be varied. However, inherent in this method is relatively narrow bandwidth operation; since the direction the array antenna points is, by design, a function of frequency.

Another form of phase control is effected by the construction of an antenna having a multiplicity of RF input ports, each of which is connected corporately to the total number of radiating elements in such a way that the radiated beam points in a unique direction when fed at one

particular port. Beam scanning, then, is affected by switching the transmission power from one port to another. In this case, a large number of transmitter tubes is necessary unless the transmitter energy can be switched between the various antenna input ports. Then the accomplishment of super high power radars of this form is dependent upon successful development of appropriate high speed, high power microwave switches.

The RF power capability of switches and microwave phase shifters can be shown commensurate for typical applications. This suggests, then, that antenna pointing might be affected in a more direct manner using microwave phase shifters which are individual to separate antenna elements or groups of antenna elements. Such microwave phase shifters take the form of a two-port transmission network whose propagation constant is conveniently controlled.

Recommended microwave phase control networks have included the use of electro-mechanical and electro-hydraulic, ferrite, and semiconductor elements. Though the salient features and disadvantages of each are indeed unique, they vary distinctly by virtue of the speed at which control can be effected.

Electro-mechanical or hydraulic devices typically have control times of the order of milliseconds. The properties of ferrite materials may be varied by the application of a magnetic field and such control usually is accomplished in tens to hundreds of microseconds.

Semiconductor devices are inherently much faster in their response since their properties can be varied with the application of a

bias current or voltage directly, and this control is easily effected in one microsecond with switching times considerably below 100 nanoseconds accomplishable under some circumstances.

High power phase shifting application is performed well by semiconductor PIN diodes which effect phase control through discrete switching from a low impedance at forward bias, typically less than 1 ohm of resistance, to a high impedance at reverse bias, typically greater than 100 ohms of capacitive reactance in the L-band frequency range. Since the control element essentially varies as an on-off device, variations in its impedance resulting from manufacturing reproducibility, changes in temperature, or changes in applied RF power are usually insignificantly small; and highly desirable distortion-free, reproducible operation can be obtained.

B. Low Power Phase Shifting

Applications which require microwave phase control at low power levels include countermeasure networks, driver stages in high power parallel chain amplifier circuits, and automatic, microwave impedance measuring, bridge circuits. Within a countermeasure circuit, an enemy signal may be phase modulated with random or deceptive information and be transmitted to its original source. In this way, accurate target velocity determination by interpretation of the return signal frequency deviation or phase change can be inhibited.

Within a high power amplifier chain, a microwave phase shifter may be used to control the phase of low level driver stages in order to

keep in synchronism the output of parallel microwave high power tubes, that are used in conjunction, for the generation of higher power than can be obtained with single tubes. A further advantage of this controlled phase, parallel tube, high power generation technique is that it also can be used for switching the resultant microwave energy. Typically, for example, this might be accomplished with two tubes by feeding their output power into separate ports of a 90° hybrid coupler. The combined energy can then be made to exit from either of the coupler's remaining two ports according to the relative phase between the two input signals.

In an automatic, microwave impedance measuring, bridge circuit, a phase shifter may be used to produce at high speed a calibrated phase shift in the known impedance arm, permitting instantaneous measurement of a rapidly varying unknown microwave impedance.

In these low power phase shift applications, semiconductor varactor diodes may be used to yield large ranges of continuous phase shift. In such circuits, the varactor impedance is essentially capacitively reactive and varies in a continuous manner according to an applied bias. If the applied microwave voltage is small compared to the bias, then the diode impedance, and hence the phase shift obtained, is determined only by the bias voltage, and distortion-free operation is obtained. Typically, in 50 ohm transmission systems, the RF level for distortion-free operation is less than 1 watt, although operation to higher levels may be extended where some change in the phase shift versus bias characteristic with increasing power is not objectionable.

The advantage gained by using varactors when the RF power level is low in the phase shift design is that wide phase shift ranges with relatively few diodes may be achieved. Single continuous phase shifting devices have been built to yield about 250° of phase shift per decibel of insertion loss per kilo-megacycle of operating using 170 Kmc cut-off diodes; as much as 270° of phase shift was obtained using two varactor diodes, only one diode would be necessary if a circulator were to replace the hybrid coupler used in the balanced circuit tested.

High power operation of continuous phase shifters was studied, under Contract N0bsr-81470, using special varactor diodes having breakdown voltages exceeding 500 volts. However, the variation of phase shift with operating RF power level was judged to be a serious restriction on the ultimate usefulness of this continuous phase shifter form; and, therefore, no further efforts were performed to operate at high power with continuous type varactor diode phase shifters.

III TRANSMISSION-REFLECTION MODE

A. CIRCUIT CONFIGURATION

1. Matched Transmission Requirements

The transmission-reflection phase shifter circuit can be made to have matched two-port characteristics that are independent of its phase shift characteristics by employing the directive properties of a circulator or hybrid coupler. Control of the phase difference between input and output waves is effected, then, using terminations for the directive circuit whose reflection coefficient has near unity magnitude but controllable phase. These circuits are depicted in Figure (1). Use of the circulator approach yields a circuit whose phase shift is non-reciprocal between input and output terminals. The hybrid coupler circuit of Figure (1-b) requires a pair of symmetric controllable terminations, but possesses reciprocal operation. In addition, the matched transmission bandwidth of the hybrid coupler circuit can be achieved for bandwidths of an octave or more.

Hybrid couplers with matched impedances at all ports have been analyzed in detail by Cohn, Sherk, Shimizu, Jones, Bolljahn, Oliver and many others. From these results, the reflection coefficient experienced at the input of a hybrid coupler symmetrically terminated with reflection coefficients, Γ , may be calculated as shown in Figure (2).

The maximum $VSWR_{in}$ resulting from symmetric, unity magnitude reflection coefficients, Γ , at the "3 db ports" is shown plotted in Figure (3) with the center frequency power coupling ratio, k^2 , as parameter. Experimental versus theoretical performance of a 2.7 db hybrid

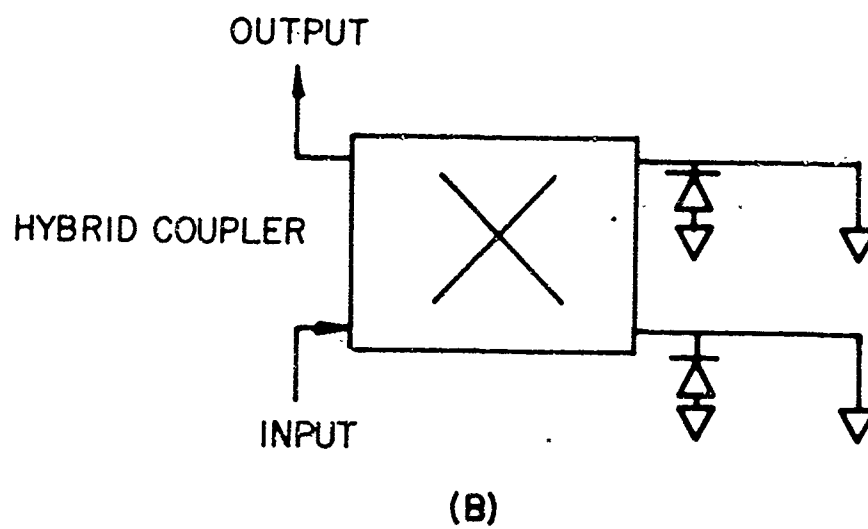
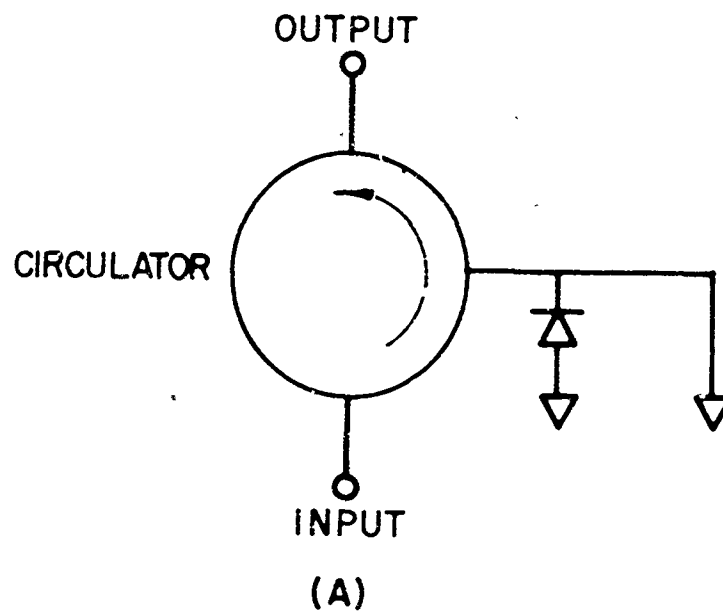
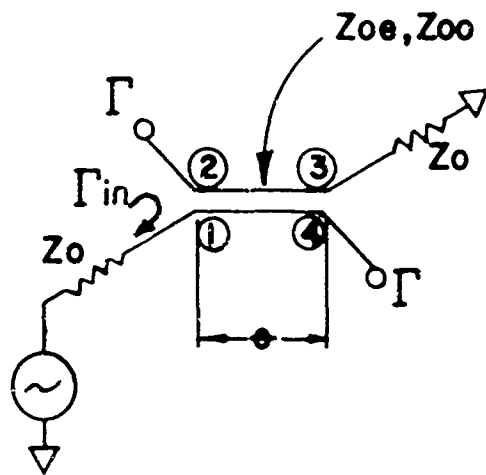


FIGURE 1
TRANSMISSION-REFLECTION PHASE SHIFTERS



Z_{oo} = odd mode impedance

Z_{oe} = even mode impedance

$$Z_o = \sqrt{Z_{oe} Z_{oo}}$$

$Z_o = 1$ (normalized)

$$k = \frac{Z_{oe} - Z_{oo}}{Z_{oe} + Z_{oo}}$$

SCATTERING EQUATION: $b = sa$

$$S = \begin{bmatrix} 0 & f_1 & 0 & f_2 \\ f_1 & 0 & f_2 & 0 \\ 0 & f_2 & 0 & f_1 \\ f_2 & 0 & f_1 & 0 \end{bmatrix}$$

$$f_1 = \frac{jk \sin \theta}{\sqrt{1-k^2} \cos \theta + j \sin \theta}$$

$$f_2 = \frac{\sqrt{1-k^2}}{\sqrt{1-k^2} \cos \theta + j \sin \theta}$$

$$|\Gamma_{in}| = \left| \Gamma \frac{1-k^2 (\sin^2 \theta + 1)}{(\sqrt{1-k^2} \cos \theta + j \sin \theta)^2} \right|$$

$$VSWR_{in} = \frac{1 + |\Gamma_{in}|}{1 - |\Gamma_{in}|}$$

FIGURE 2

REFLECTIVELY TERMINATED HYBRID COUPLER EQUATIONS

$$|\Gamma| = 1$$

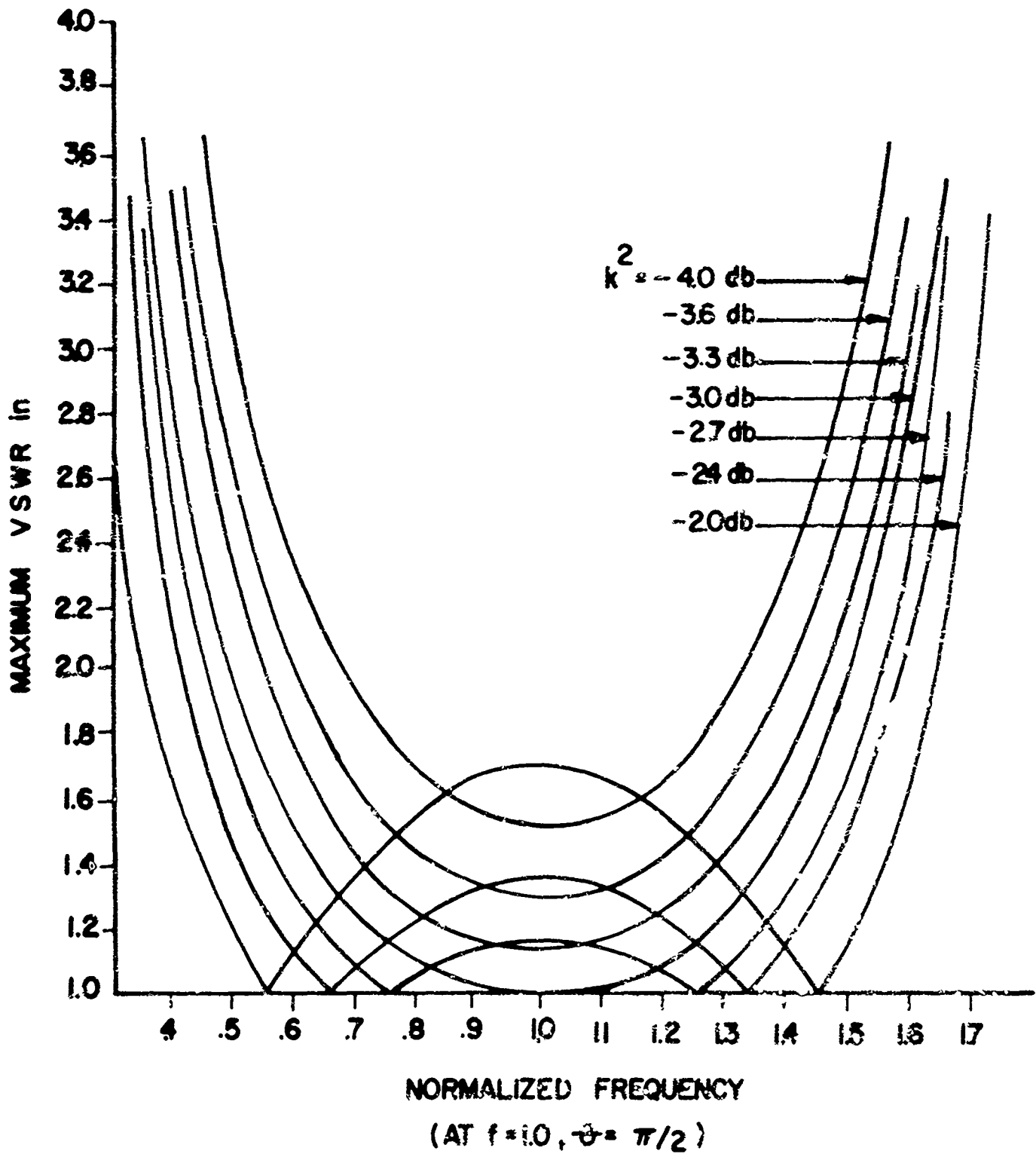


FIGURE 3

THEORETICAL VSWR Γ IN VERSUS FREQUENCY CHARACTERISTIC
OF A REFLECTIVELY TERMINATED HYBRID COUPLER

coupler so terminated by symmetric open circuits is shown in Figure (4).

2. Controlled Reflection Terminations

Either continuous or discrete increment control of the termination reflection coefficient may be effected accordingly as varactor or PIN diodes are used as control elements in the termination, Fig. 5. In Figure (6) is shown the relative change of reflection coefficient phase as a function of the normalized variable capacitive susceptance, B , of a continuously controlled termination with the short circuited terminating line length as parameter. A termination using two varactor diodes together with its phase shift versus normalized capacitive susceptance characteristic is shown in Figure (7). More than 360° of phase shift in principle is obtainable from this circuit. Experimental results were obtained for the single diode termination and are described in the next section.

Although continuous phase shift is attractive, its implementation with varactor diodes typically is limited to very low power levels, of the order of milliwatts. This occurs because the capacity of the varactor is a function of the instantaneous voltage applied to it. Thus, to prevent distortion of the phase shift versus bias characteristic as well as attendant harmonic generation, the RF voltage applied must be very small compared to the control bias voltage. For this reason, the discrete increment phase shifter using a PIN switching diode is desirable for linear high power operation. In this case, depicted as Figure (5-b), the phase shift is equal approximately to twice the length of

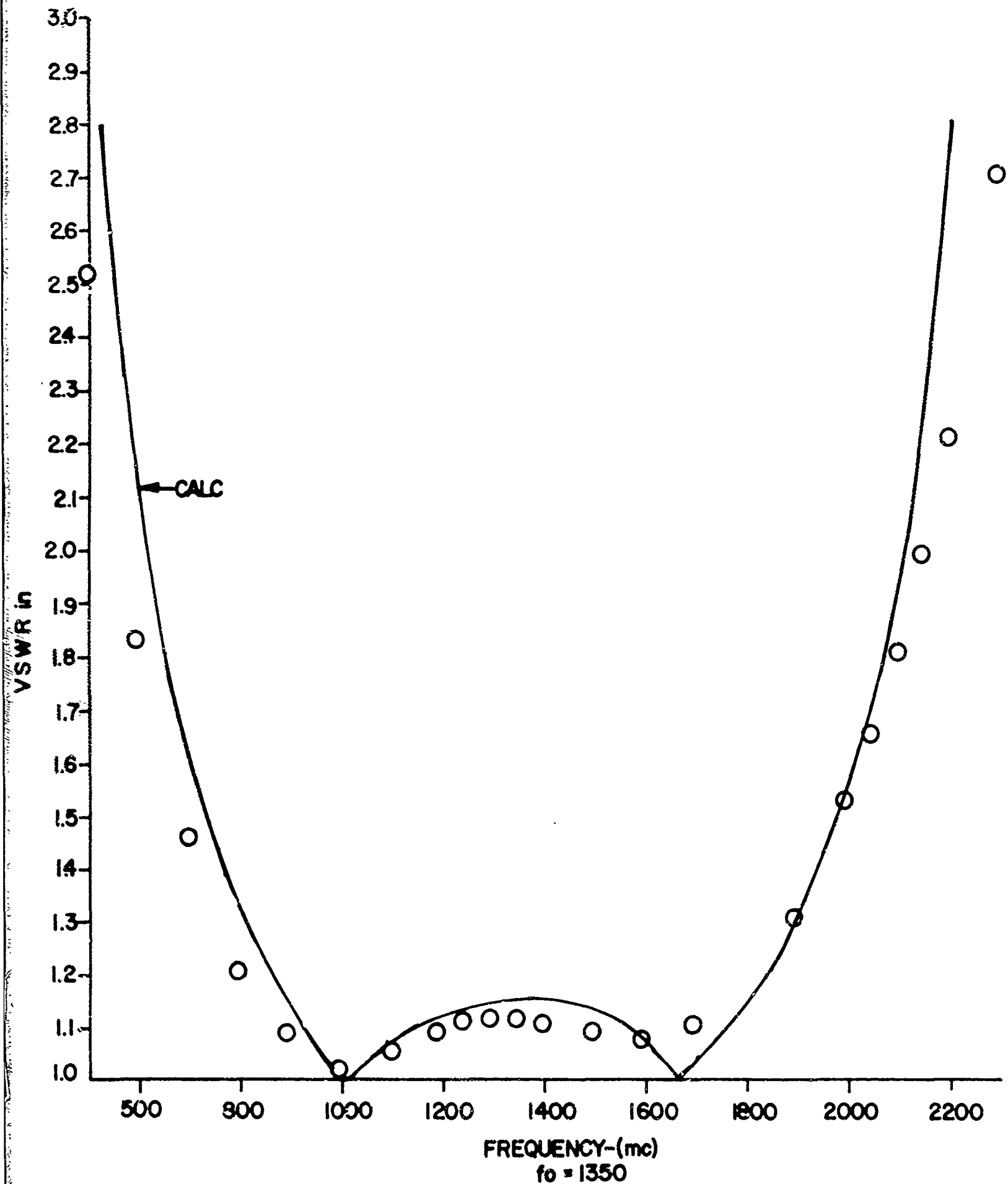
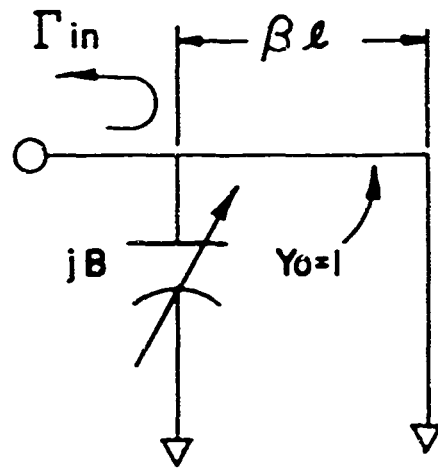
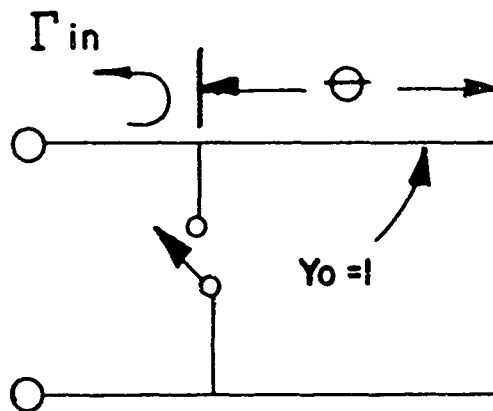


FIGURE 4

MEASURED AND CALCULATED VSWR IN SYMMETRIC OPEN CIRCUIT TERMINATED HYBRID COUPLER



(A) VARACTOR DIODE TERMINATION EQUIVALENT CIRCUIT



(B) PIN DIODE TERMINATION EQUIVALENT CIRCUIT

FIGURE 5

CONTROLLED REFLECTION TERMINATIONS

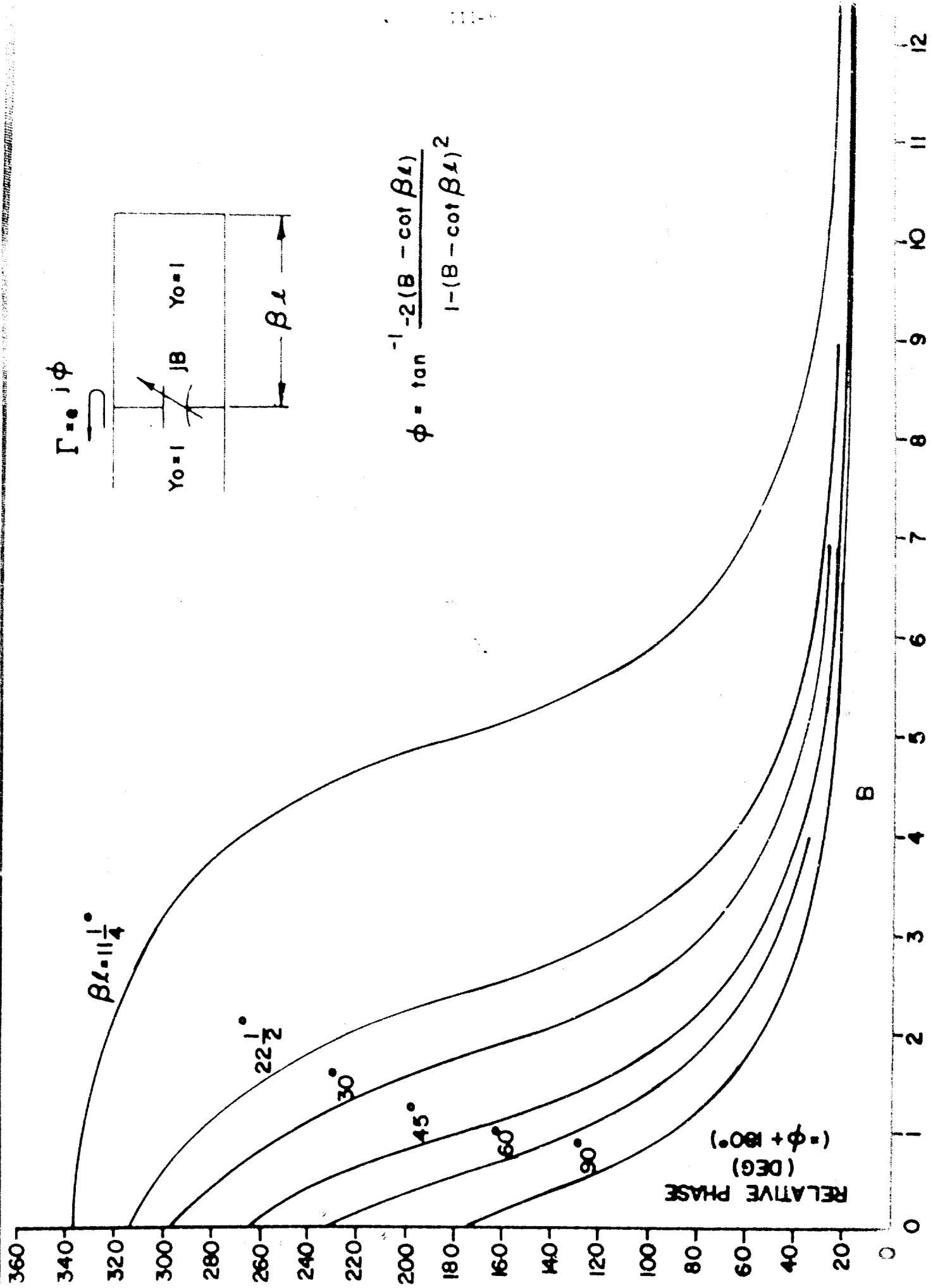


FIGURE 6

CONTINUOUSLY PHASE VARIABLE, SINGLE VARACTOR TERMINATION

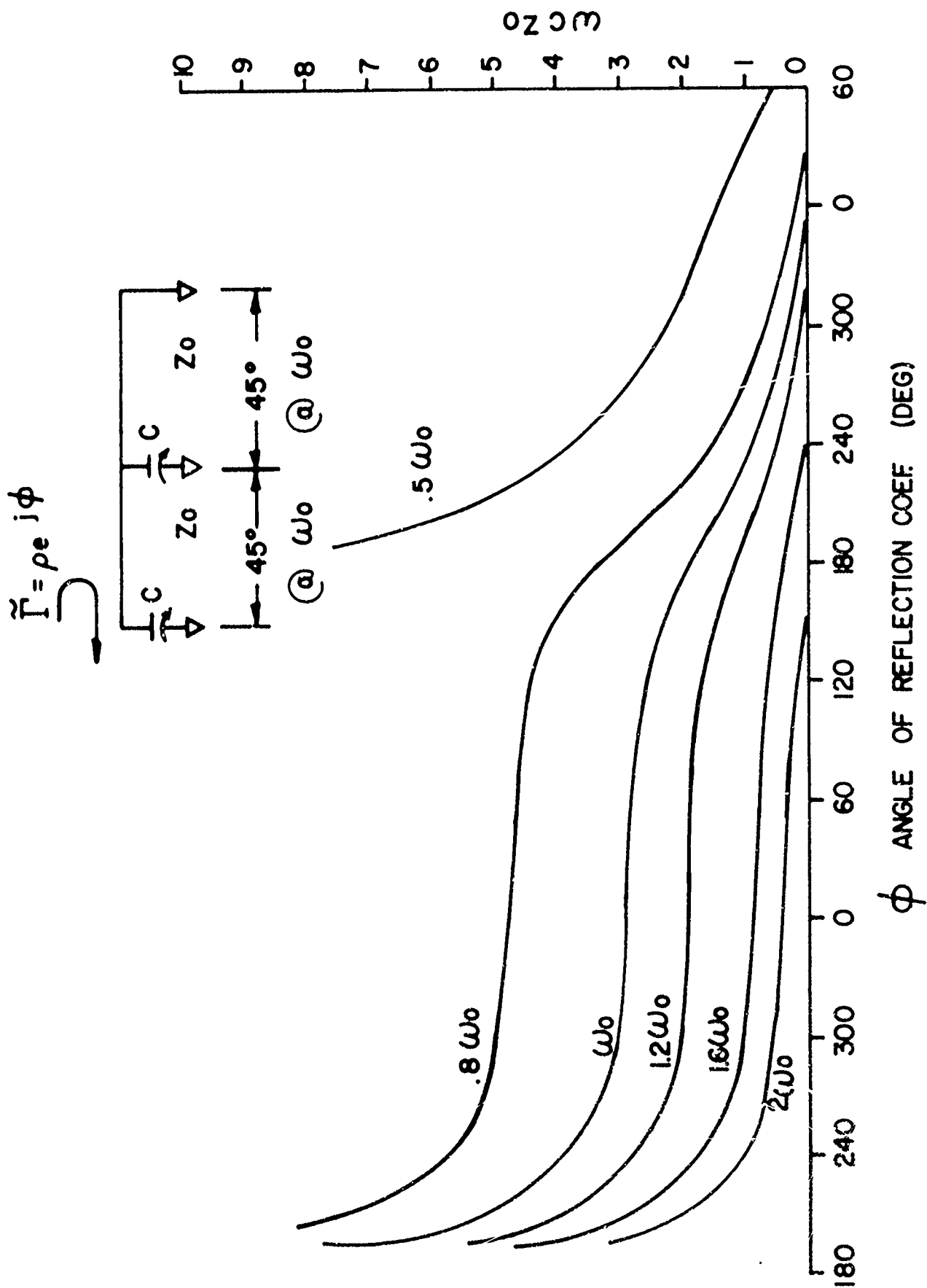


FIGURE 7

CONTINUOUSLY PHASE VARIABLE, TWO VARACTOR TERMINATION

short circuited line switched and, in principle, has a magnitude proportional to frequency if a nondispersive line length, θ , is used.

B. CIRCUIT IMPLEMENTATION

1. The Continuous Phase Shifter

a. Analytical Procedure: The circuit and phase shift characteristics shown in Figure (6) are useful for selection of approximate circuit parameter values, but a more complete equivalent circuit which includes the diode resistance and parasitic series inductance is necessary for accurate calculation of the termination's phase shift and insertion loss. The parameters of an experimental varactor termination are shown in Figure (8) and the resulting admittance plot of the termination is shown in Figure (9) for an operating frequency of 1,000 mc. At this frequency, the diode package capacity, approximately 0.3 pf, has been lumped into the total diode capacity, C. A plot of C versus applied bias voltage for both of the diodes used in the symmetric termination pair is also included in Figure (8).

b. L-Band Model: A pair of terminations whose calculated admittance versus control bias for the included varactor diode is shown in Figure (9), was used at the output of a 3 db hybrid coupler and the measured and calculated values of phase shift may be seen compared in Figure (10). These agree closely at 1000 Mc with somewhat larger discrepancies between measured and calculated phase shift versus bias characteristics at the higher frequencies 1500 Mc and 2000 Mc. This may have resulted because the length of the short circuit line used as a

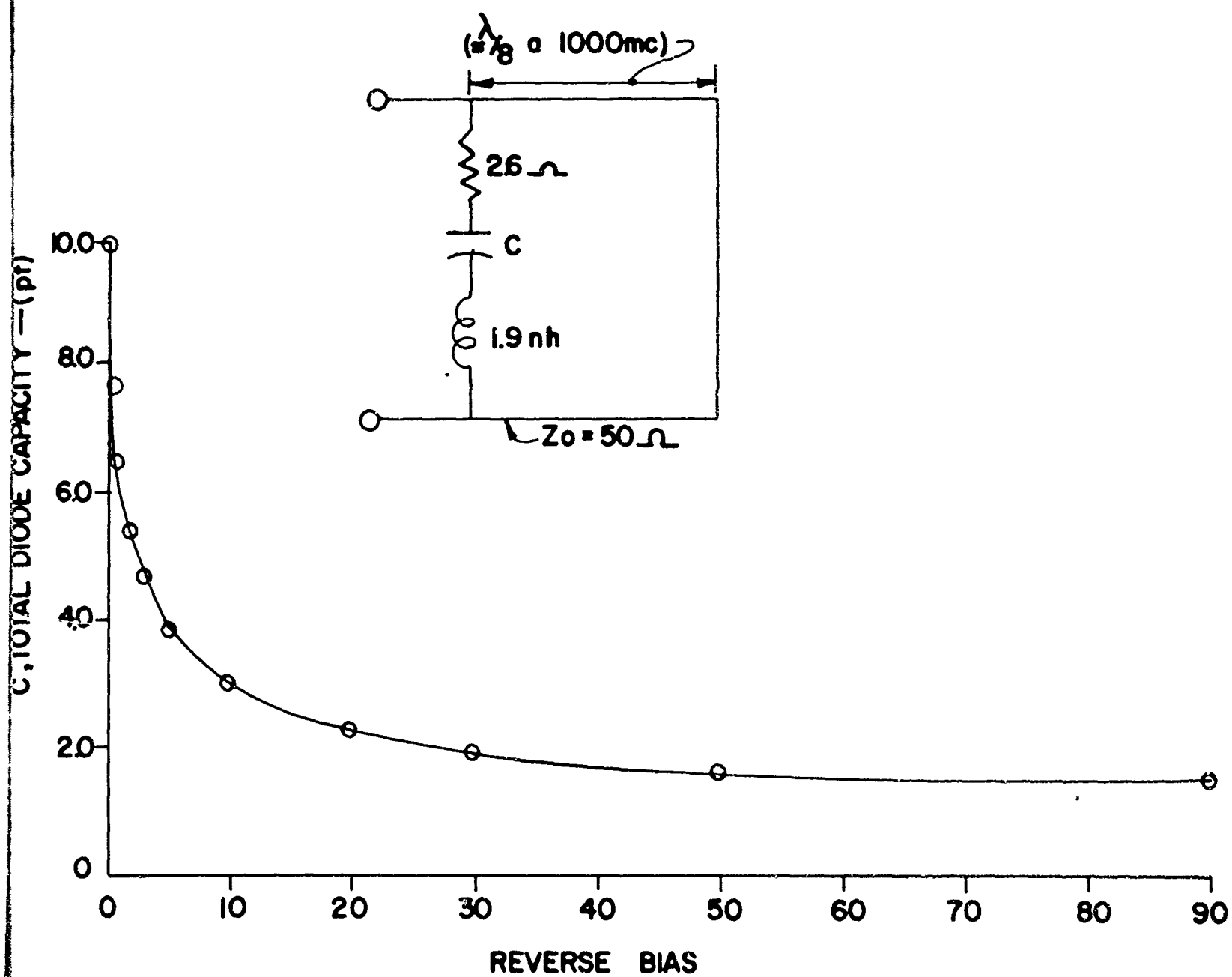


FIGURE 8

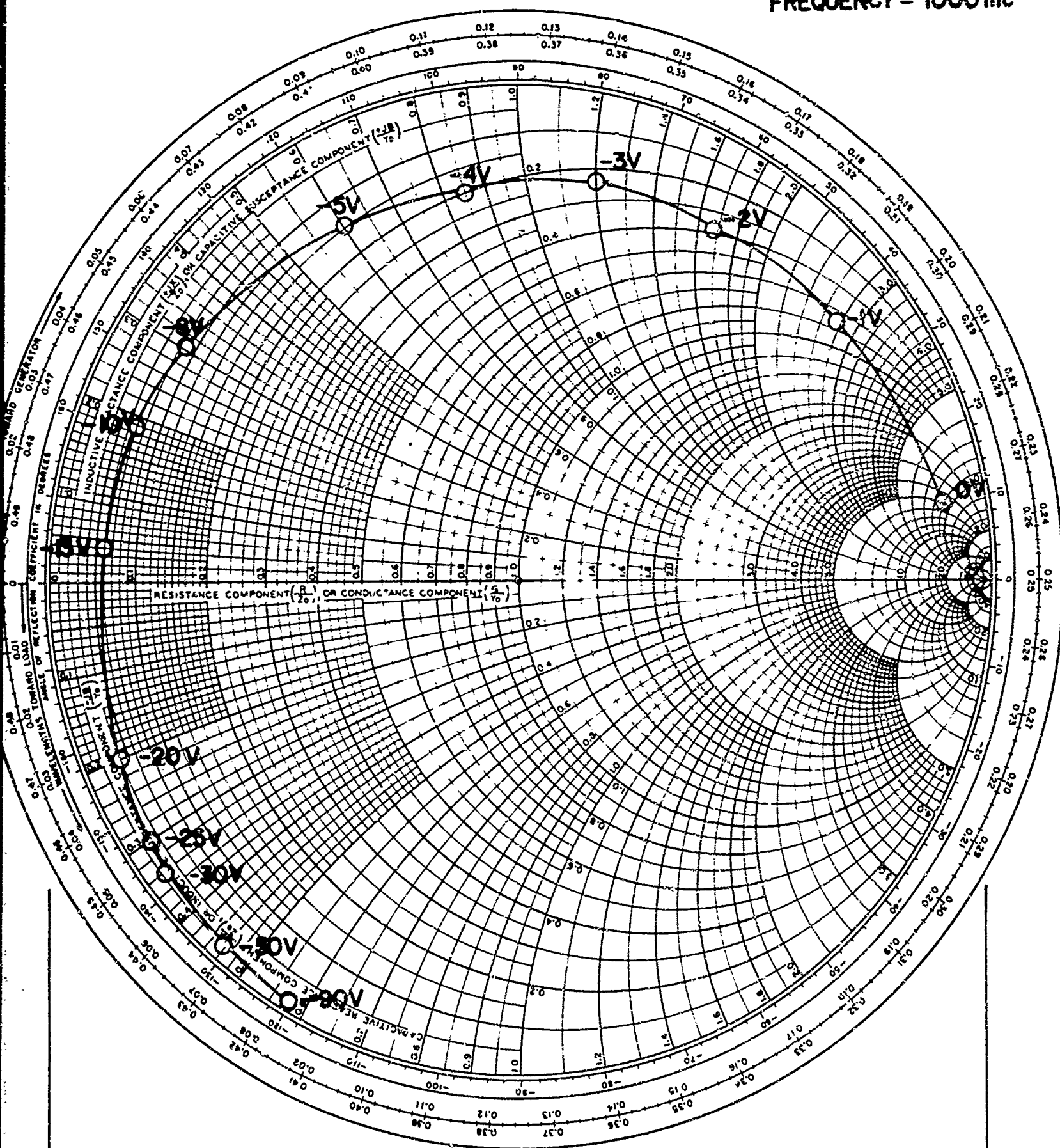
VARACTOR TERMINATION PARAMETERS

FIGURE 9 III-12

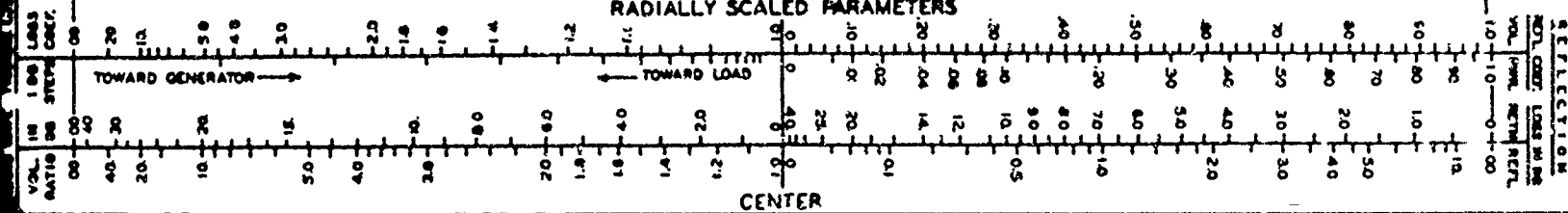
NAME	TITLE	DWG. NO.
SMITH CHART FORM 756-N	VARIABLE TERMINATION ADMITTANCE PLOT MICROWAVE ASSOCIATES BURLINGTON, MASS.	DATE

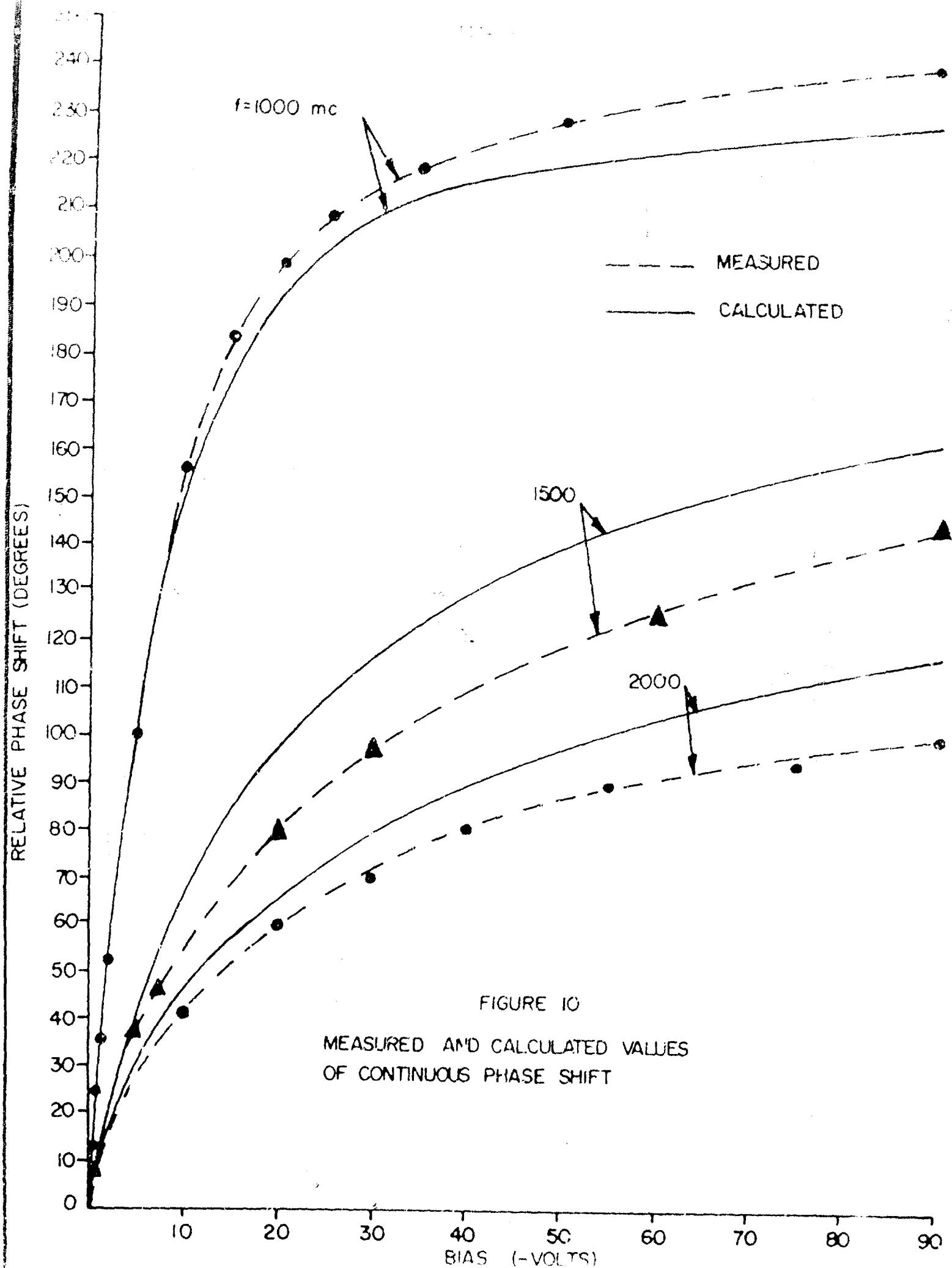
ADMITTANCE COORDINATES

FREQUENCY = 1000 mc



RADIALLY SCALED PARAMETERS





back-up for the shunt mounted diode is known only approximately. A spring finger sliding short circuit had been used to terminate the line and the exact location of the short circuit, as well as the characteristic impedance of the line in the vicinity of the short circuit fingers, are known only approximately.

The insertion loss of the continuous phase shifter over the L-band frequency range is shown plotted in Figure (11). In all cases examined, the frequency for which the maximum phase shift resulted was also that at which the maximum insertion loss was obtained. In this case, the maximum loss measured at 1000 Mc was 2.1 decibels. The measured phase shift was about 240° . Considering that the circuit losses with diodes removed were of the order of 0.3 decibels, the figure of merit for the diodes as used in this configuration was approximately 135° of phase shift per decibel of insertion loss.

More phase shift per decibel of insertion loss would be expected from diodes with higher cut-off frequencies. The results just described were achieved with diodes whose cut-off frequency measured at the 90 volt breakdown voltage was 41 Kmc. This is calculated using the series resistance value 2.6 ohms and the voltage breakdown capacity of 1.5 picofarads. Within the last quarter, higher cut-off frequency diodes were used in an L-band phase shifter circuit. Measurements were made at 1800 Mc since the input VSWR to this particular coupler was minimal at this frequency.

The measured phase shift and insertion loss may be seen

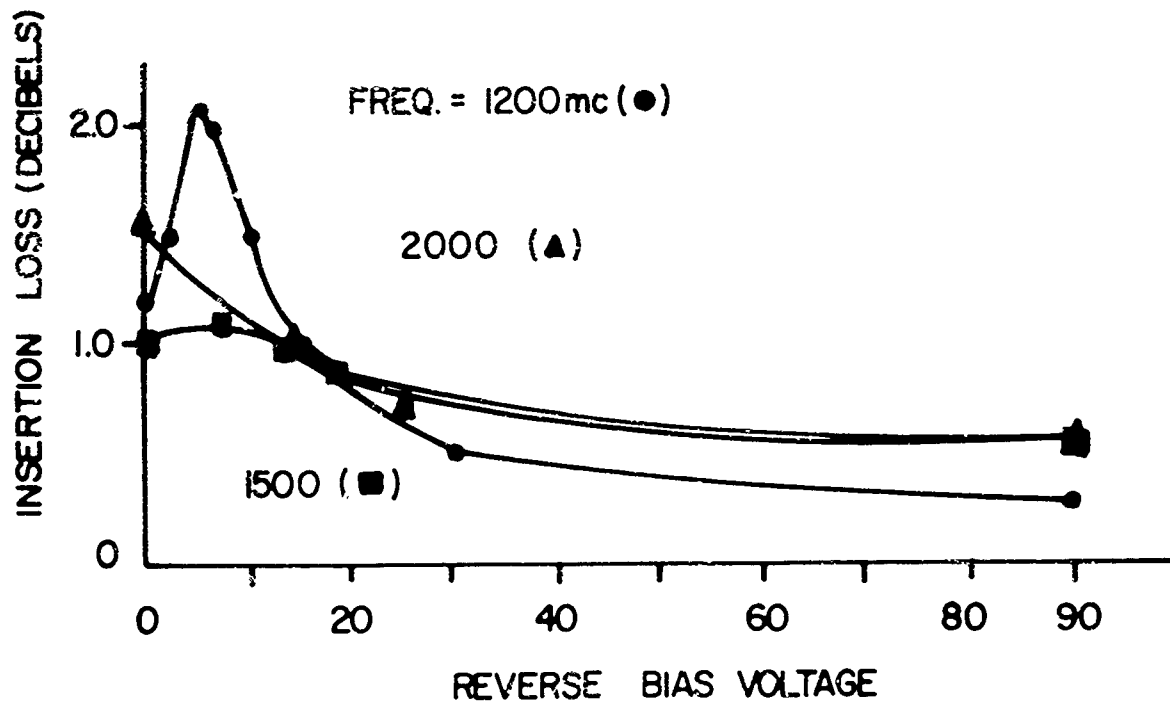


FIGURE II

INSERTION LOSS VERSUS BIAS
OF CONTINUOUS PHASE SHIFTER

plotted in Figure (12). A maximum of 184° of phase shift was obtained while the maximum insertion loss did not exceed 1.1. If, again, 0.3 db is subtracted to account for the circuit losses, the figure of merit for this phase shifter was about 230° of phase shift per decibel of insertion loss. This was also achieved at a higher operating frequency, 1800 Mc, compared with the previous 1000 Mc. If the figure of merit is made proportional to the operating frequency, then these results yield about 415° of phase shift per decibel of insertion loss per kilo-megacycle. The diodes used had a capacity variation of 4.5 picofarads at zero bias to 0.9 picofarads at breakdown, 60 volts. The series resistance was very nearly 1 ohm and, thus, the cut-off frequency of these diodes was about 175 Kmc. From these results, it can be seen that the phase shifter figure of merit was nearly proportional to the cut-off frequency of the diodes used.

c. S-Band Model: Also within the last quarter, an S-band continuous phase shifter was constructed and tested at 2800 Mc using the same 5 picofarad diode pair quoted for the 1800 Mc performance. The results obtained may be seen in Figure (13). 190° of phase shift was achieved with a maximum insertion loss of 1.4. Again, if about 0.3 decibels of loss are attributable to the circuit, then the phase shifter figure of merit is about 485° phase shift per decibel of insertion loss per kilo-megacycle. Considering that the insertion loss allowance for the circuit with diodes removed may not in all cases be the same, these results are in fairly close agreement. A figure of merit may be then

FREQUENCY = 1800mc

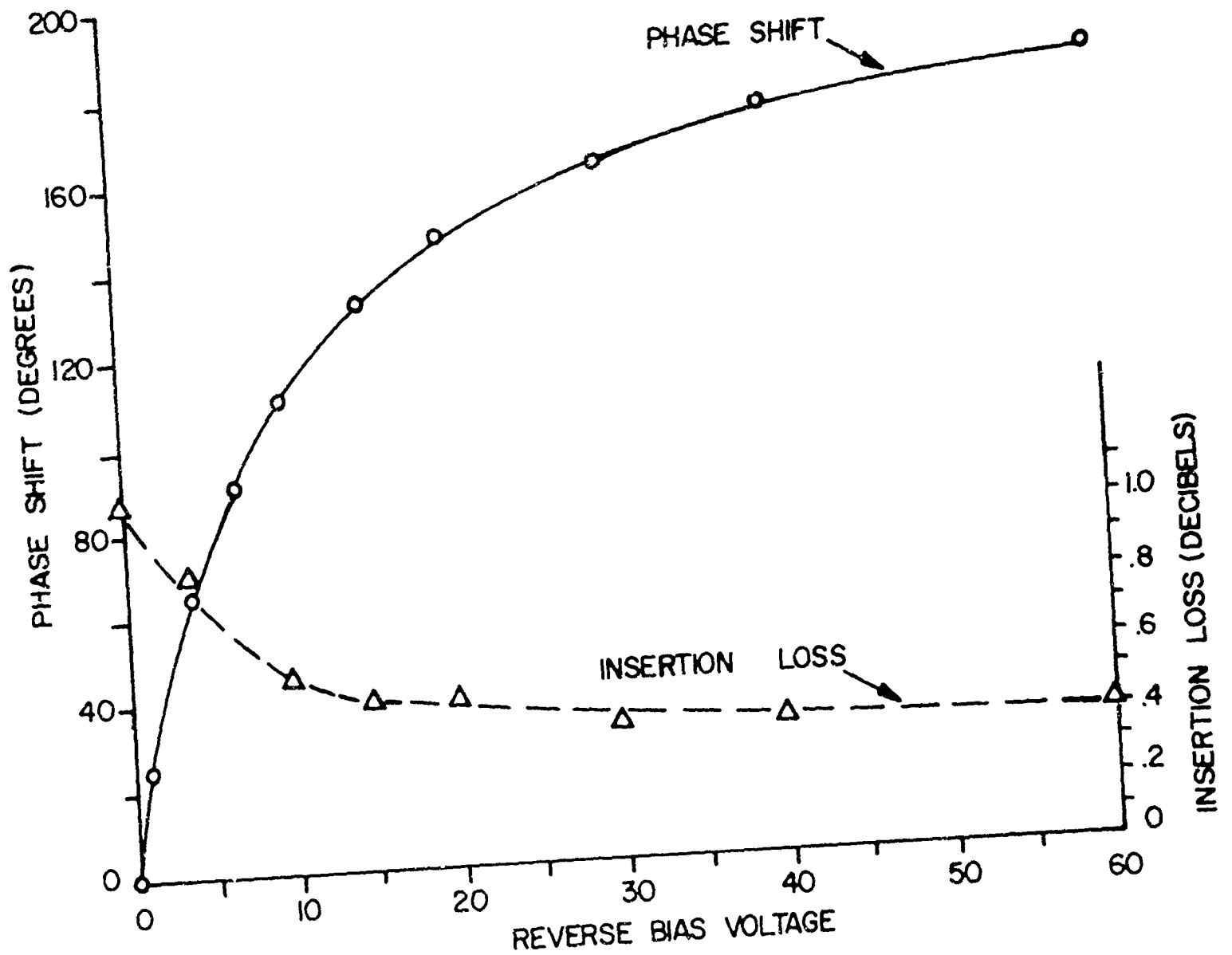


FIGURE 12

PHASE SHIFT AND INSERTION LOSS OF
L-BAND PHASE SHIFTER

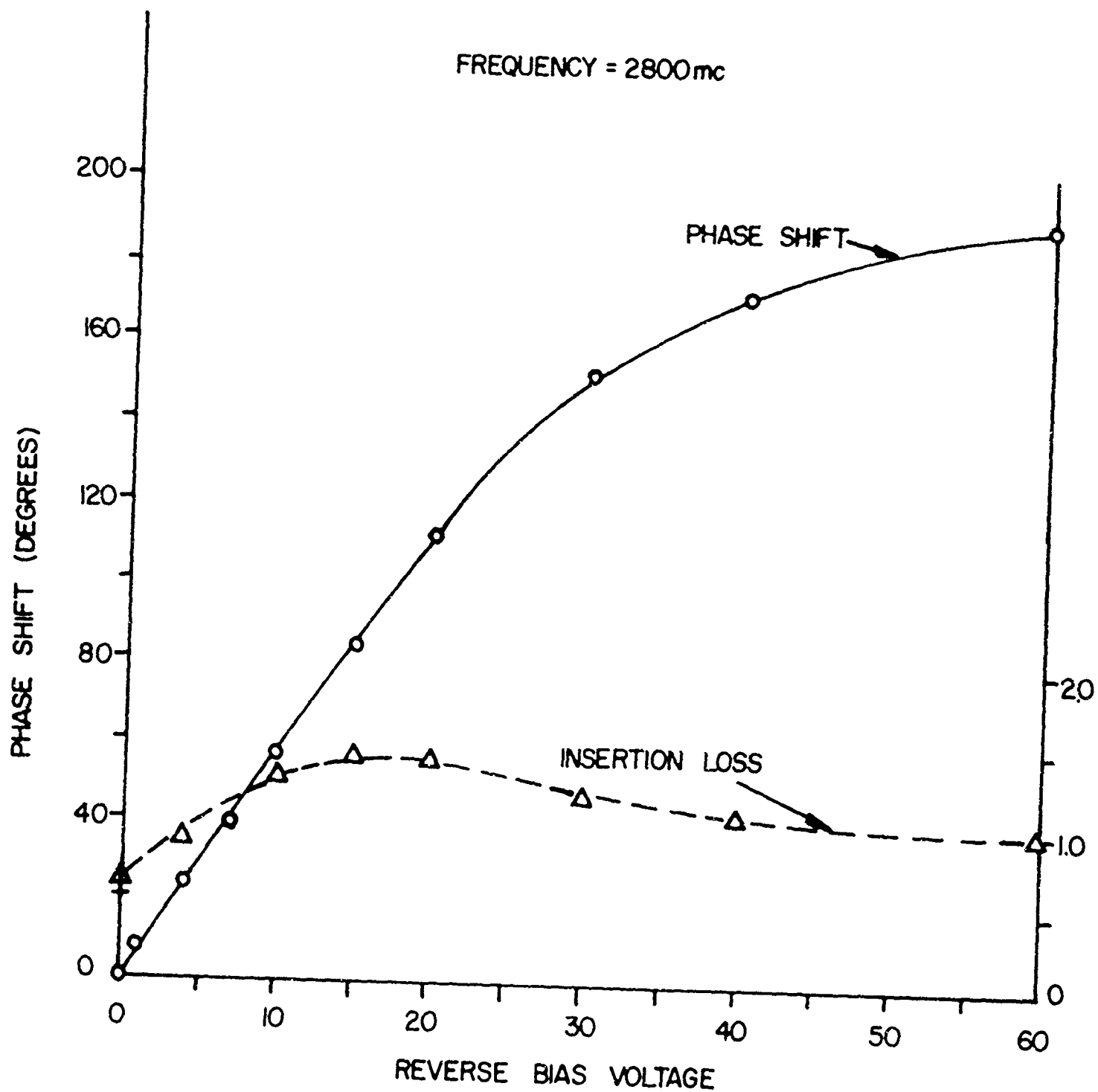


FIGURE 13

PHASE SHIFT AND INSERTION LOSS OF
S-BAND PHASE SHIFTER

defined for continuous phase shifters in the L and S frequency bands which use varactor diodes having capacity values in the 1 - 10 picofarad range and are adjusted to yield phase shift increments of about 200° . This indicates that the empiric relationship of Figure (5) can be used with good approximation to estimate the inter-related phase shift, insertion loss, operating frequency, and diode figure of merit -- the cut-off frequency.

$$F = \frac{\Delta\phi}{I.L.} \approx \frac{4 \text{ (Degrees)}}{\text{(Decibel)}} \times \frac{\text{(Diode Cut-off Frequency)}}{\text{(Operating Frequency)}}$$

Equation (1)

d. RF Power Limitations: The continuous phase shifter using varactor diodes is limited to low RF power levels. The first limiting factor is the variation of the diode capacity with the applied RF voltage. This is very undesirable because at RF power levels appreciably larger than 1 watt, the phase shift versus bias characteristic becomes a function of the operating power. This result may be seen plotted in Figure (14); it was first discussed in the Second Quarterly Progress Report. Even if this distortion of the phase shift characteristic is tolerable, the effect of diode rectification inhibits operation of the phase shifter beyond RF levels of about 25 watts. These RF power ratings are based upon a 50 ohm hybrid coupler transmission reflection continuous phase shifter using diodes with reverse breakdown voltages of approximately 100 volts. This nonlinear behaviour results from the varactor diode's ability to maintain a capacity determined by the applied

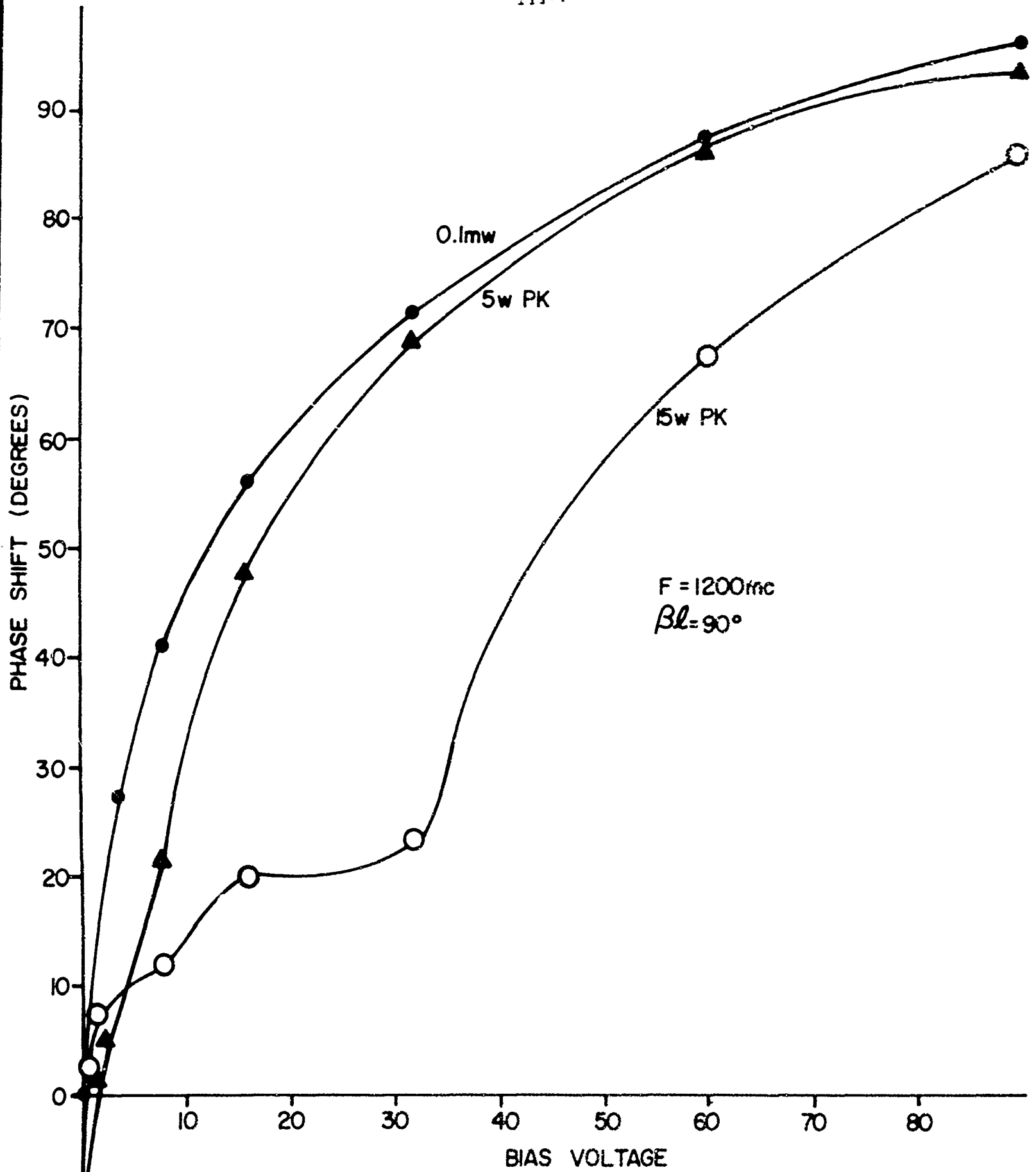


FIGURE 14

CONTINUOUS PHASE SHIFTER
4 PARALLEL MOUNT DIODES

voltage at its terminal even when this voltage varies at a microwave rate. A means for slowing down this response -- and thus a means for insuring circuit linearity with RF power -- results from the use of an intrinsic semiconductor region between the P and N regions. The resulting "PIN Diode", as will be seen, is suitable for operation at tens to hundreds of kilowatts of RF power.

e. Temperature Effects: The varactor diode capacity is not a sensitive function of temperature and, therefore, it might be expected that very little phase shift variation would occur as a function of ambient temperature for the phase shifter models described. Experimental verification may be seen in Figure (15). An L-band phase shifter which yielded 185° of phase shift at an ambient temperature of 30°C . was measured to have 189° of phase shift at 80°C . Thus, less than a 2% variation of phase shift occurred over a 50°C . temperature excursion. A portion of this phase shift variation might be expected merely from the expansion from the circuit parts, particularly the short circuit line length located behind each diode. This essentially invariant characteristic of phase shift with temperature for the continuous phase shifter typifies and is a particularly salient feature of microwave semiconductor control devices.

2. The Step Phase Shifter

a. Analytic Procedure: Calculation of the phase shift to be expected from the hybrid coupler terminated with PIN diode switched reflections is obtained straightforwardly by considering the equivalent circuit shown in Figure (5-b). In the models to be discussed, PIN diodes

III-22
FREQUENCY = 1300mc

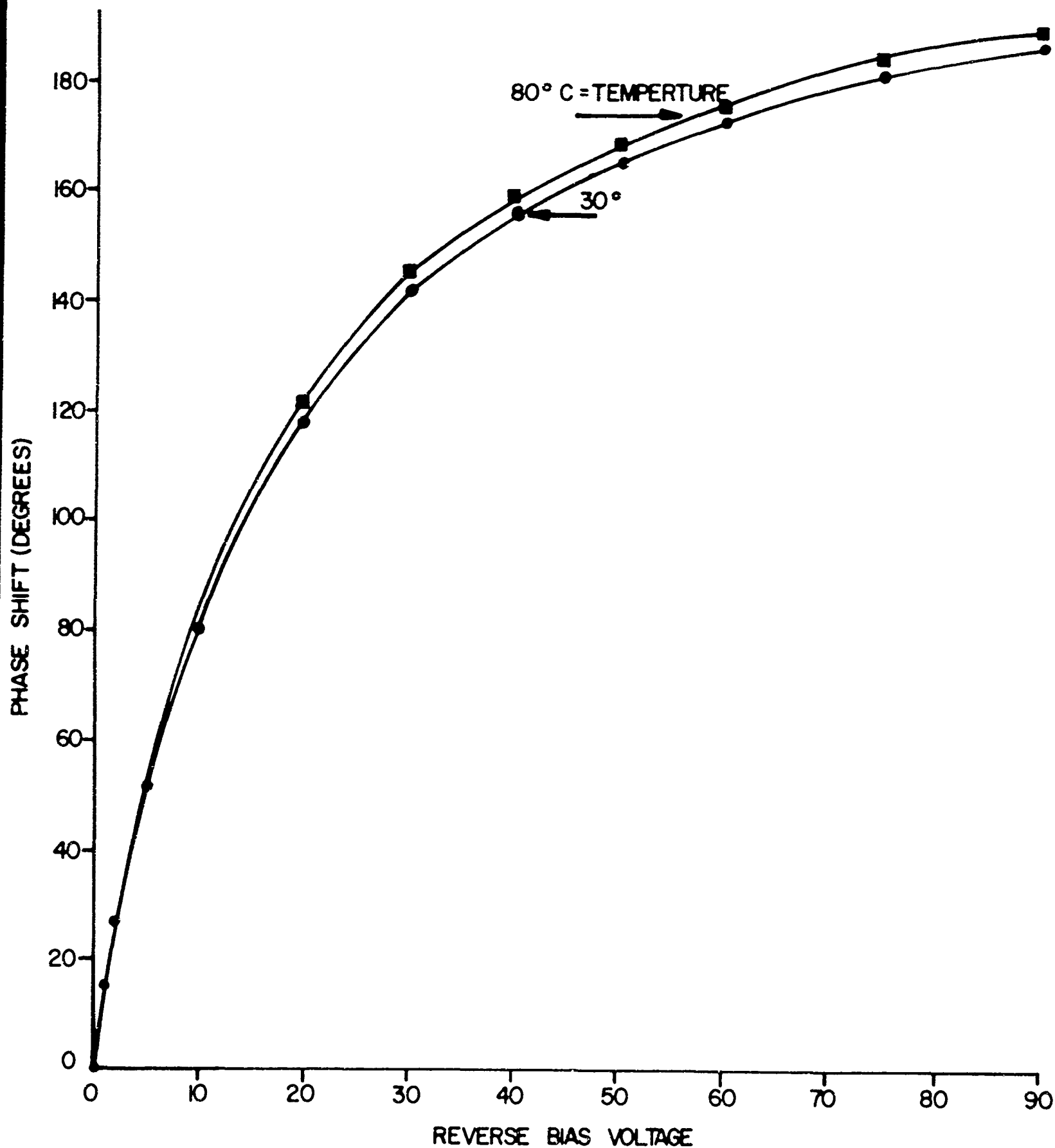


FIGURE 15

PHASE SHIFT VS BIAS WITH
TEMPERATURE AS PARAMETER

were used whose junction impedance was approximately 0.5 ohms of resistance when measured at 1000 Mc and forward biased with approximately 100 milliamperes of current. When reverse biased with -100 volts of DC bias, the RF impedance was essentially that resulting from the series combination of a 1 to 2 ohm resistance in series with about 0.8 picofarads of capacity. In all L-band models, this impedance variation was assumed to be very nearly a short or an open circuit accordingly as the diode was forward or reverse biased.

In addition to these impedance values, approximately 1 nanohenry of series inductance results in a typical diode mounting circuit. This may be attributed both to the inherent series inductance of the diode package as well as any contributions made by the circuit in which the diode is used. In all cases, this series inductance was resonantly tuned by means of a capacitor, for example, approximately 25 picofarads of capacity will series resonate 1 nanohenry of inductance at 1 kilo-megacycle. The resulting bandwidth over which this tuning was useful typically exceeds 10% to 20% in a 50 ohm characteristic impedance transmission line circuit.

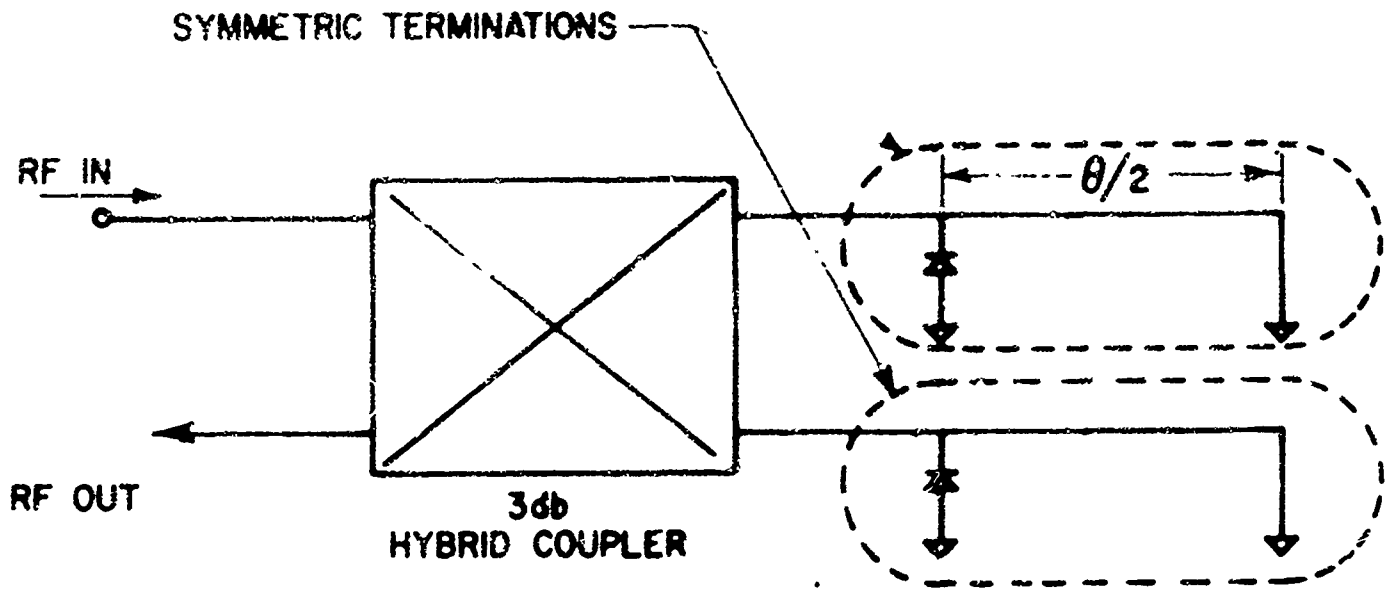
The phase shift of the terminations shown in Figure (5-b), then, is approximately equal to twice the length of short circuited line following the diode. This is considered a true time delay phase control component, and this feature is particularly desirable for use in broadband phased array antennas. In practice, phase shift proportional to frequency is achieved only approximately. Several factors

tend to inhibit the achievement of this linear phase shift versus frequency characteristic. First, the diode does not switch between a short and open circuit but rather between a reactance which may be made zero only at a center frequency by resonant tuning and a line shunting susceptance which, again, may be made zero only at a single frequency by the use of parallel resonant tuning.

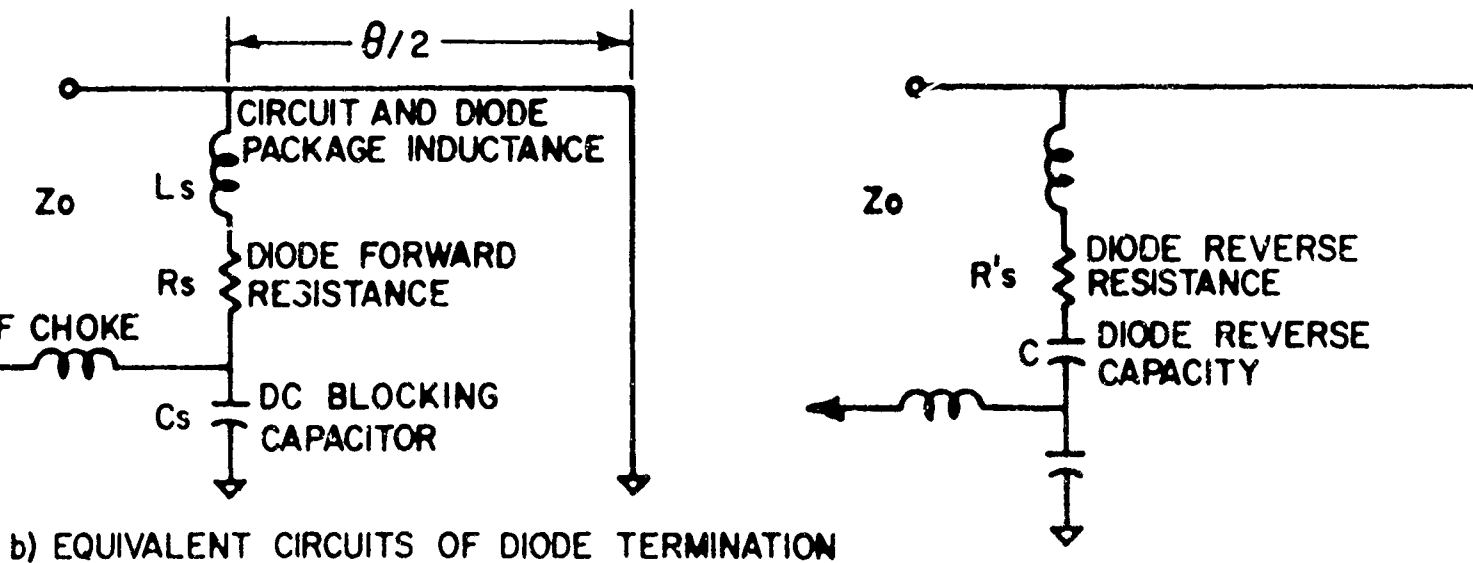
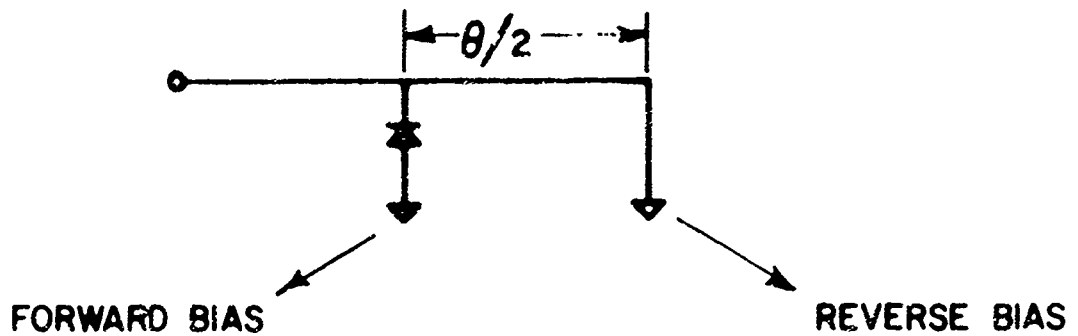
Second, the shortest length achievable for θ is limited by the proximity with which a short circuit may be placed with respect to the line shunting diode. On the other hand, long lengths for the value θ also are undesirable because they become significantly lossy. In addition, if the line length, θ , is long, then small variation in frequency produces a rapid variation of the shunt susceptance placed in parallel with the diode. Under forward bias conditions, a match condition may be achieved in which the diode's resistance, however small, may be transformed to a value near to the transmission line impedance with the result that very high insertion loss is obtained together with high energy dissipation in the controlling diode.

In this study, only the peak power handling capability achievable for phase shifters having phase shift value of 180° or less was examined.

b. L-Band Model: The equivalent circuit of the L-band model of the transmission reflection phase shifter may be seen in Figure (16). Assuming the diode to vary between short and open circuit impedances, the phase shift obtained is equal to θ , twice the length



a) TRANSMISSION-REFLECTION PHASE SHIFTER



TRANSMISSION REFLECTION PROTOTYPE
FIGURE 16

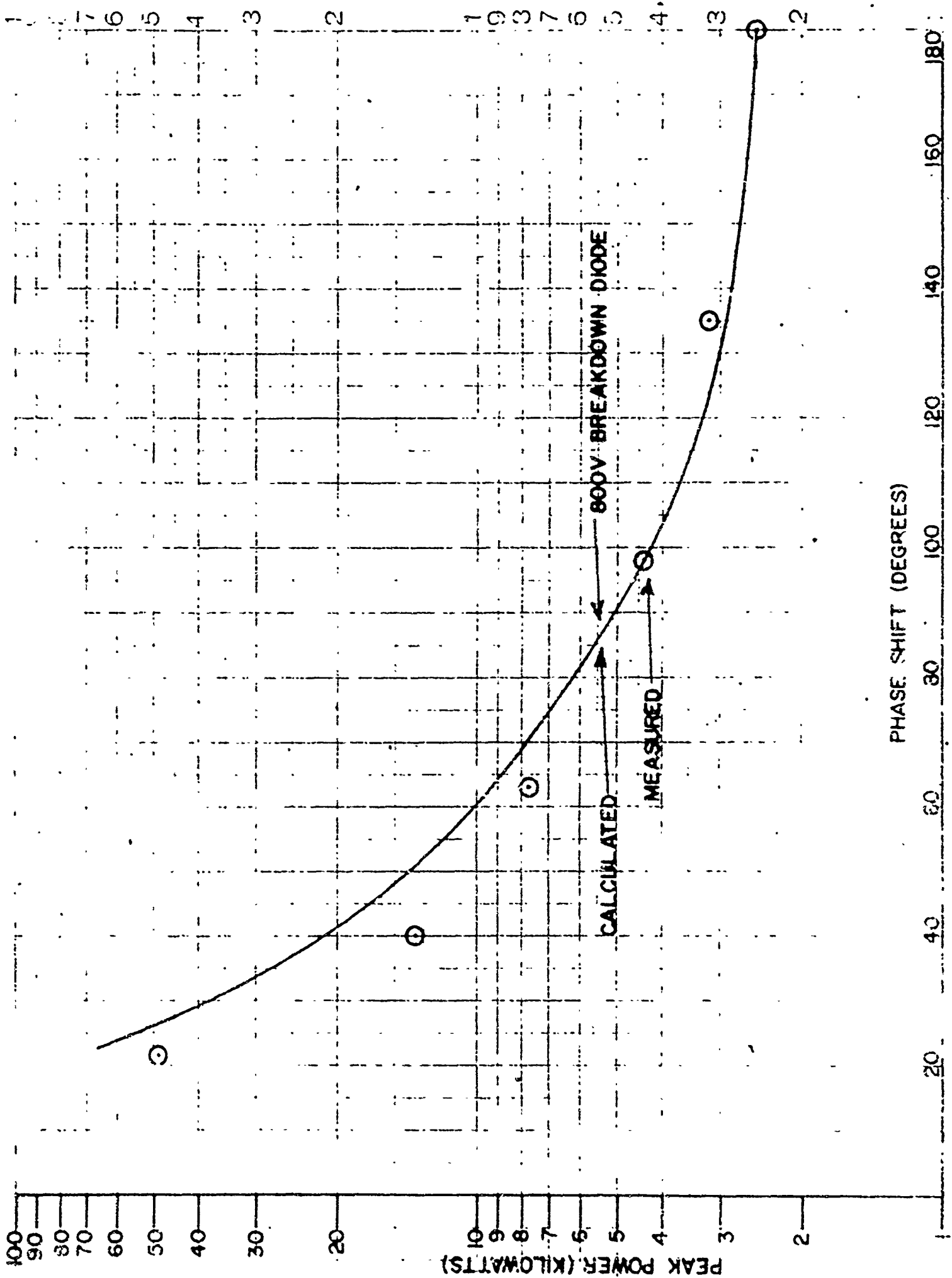
of short circuit line used in the termination. The voltage applied across the reverse biased diode is then approximately equal to $2V_L \sin(\theta/2)$. Thus, the power handling capability for the phase shifter will be related to the maximum voltage applicable to the reverse biased diode according to Equation (2).

$$P_M = \frac{V_M^2}{2Z_o} \cdot \frac{1}{\sin^2(\theta/2)} \quad \text{Equation (2)}$$

A pair of 800 volt breakdown PIN diodes was used to verify this expression. Since the maximum voltage for a given power level must be sustained by the diodes in a 180° phase shifter, the power level which the diodes sustained while drawing a reverse leakage current of about 5 microamperes each -- from which imminent breakdown could be expected -- was taken to be equal to P_M . The increase in power handling capability resulting by reducing the phase shift was then measured and compared with that which would be expected using Equation (2). These results are shown compared in Figure (17). A maximum peak power of 48 kilowatts was achieved with an RF pulse length of 5 microseconds and a duty cycle of .001 at 1300 Mc. The phase shift obtained was approximately 21.5° and the insertion loss was 0.6 decibels.

Using similar circuits, a cascade 4 bit phase shifter was constructed, that is, the phase shift achieved in the respective sections was $0 - 180^\circ$, $0 - 90^\circ$, $0 - 45^\circ$, and 0 to $22\frac{1}{2}^\circ$.* In Figure (18), the measured versus theoretical phase shift versus bias condition may be

* This work was not performed under this contract but the results are included here for completeness.



PHASE SHIFT VS. PEAK POWER OF STEP PHASESHIFTER

FIGURE 17

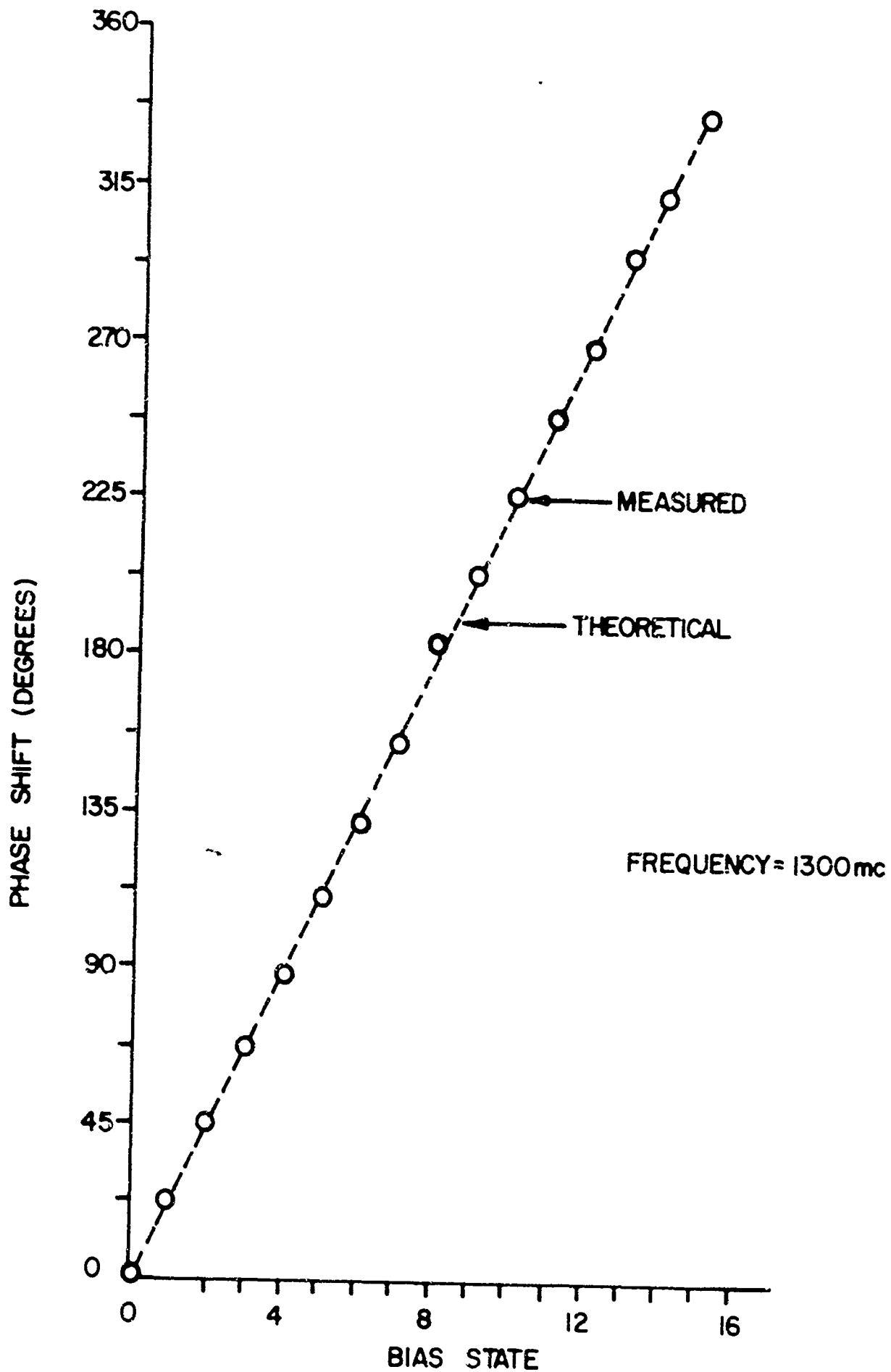


FIGURE 18

4-BIT PHASE SHIFTER VS. BIAS

seen. Fifteen values of phase shift may be obtained with a 4 bit cascade, the 0° and 360° state are considered equivalent. The maximum departure from the theoretical linear phase shift versus bias state slope was 3° .

The input VSWR to the cascade and the total insertion loss are shown in Figure (19). The maximum input VSWR was 1.4 and the mean value was 1.2. The maximum insertion loss was 1.3 decibels and the mean value was 1.6 decibels. Since diodes having approximately 800 V reverse breakdown were used, the voltage limited peak power capability of this cascade was approximately 2 kilowatts.

c. S-Band Model: A transmission reflection type S-band phase shifter was constructed. The circuit configuration, together with pertinent characteristics of the diodes used, may be seen in Figure (20). In this case, special high voltage PIN diodes were made. These consisted of a three die stack connected together internally in a single Axial Pill package. The resulting phase shift and insertion loss measurements made with the sliding short position as parameter can be seen in Figures (21) and (22) respectively. From these, it is seen that high loss behaviour is incurred for short positions between 0 and 1.25 inches. This discrepancy occurs because the diodes' series reactance is most likely not perfectly tuned at the operating frequency and the short circuit line length tends to match the diodes' resistance to the impedance of the line, resulting in high loss and unvarying phase shift. This is not a basic limitation for a multi-step phase shifter since the full range of $0 - 180^\circ$ phase shift was achieved between 1.25 and 2.25 inches.

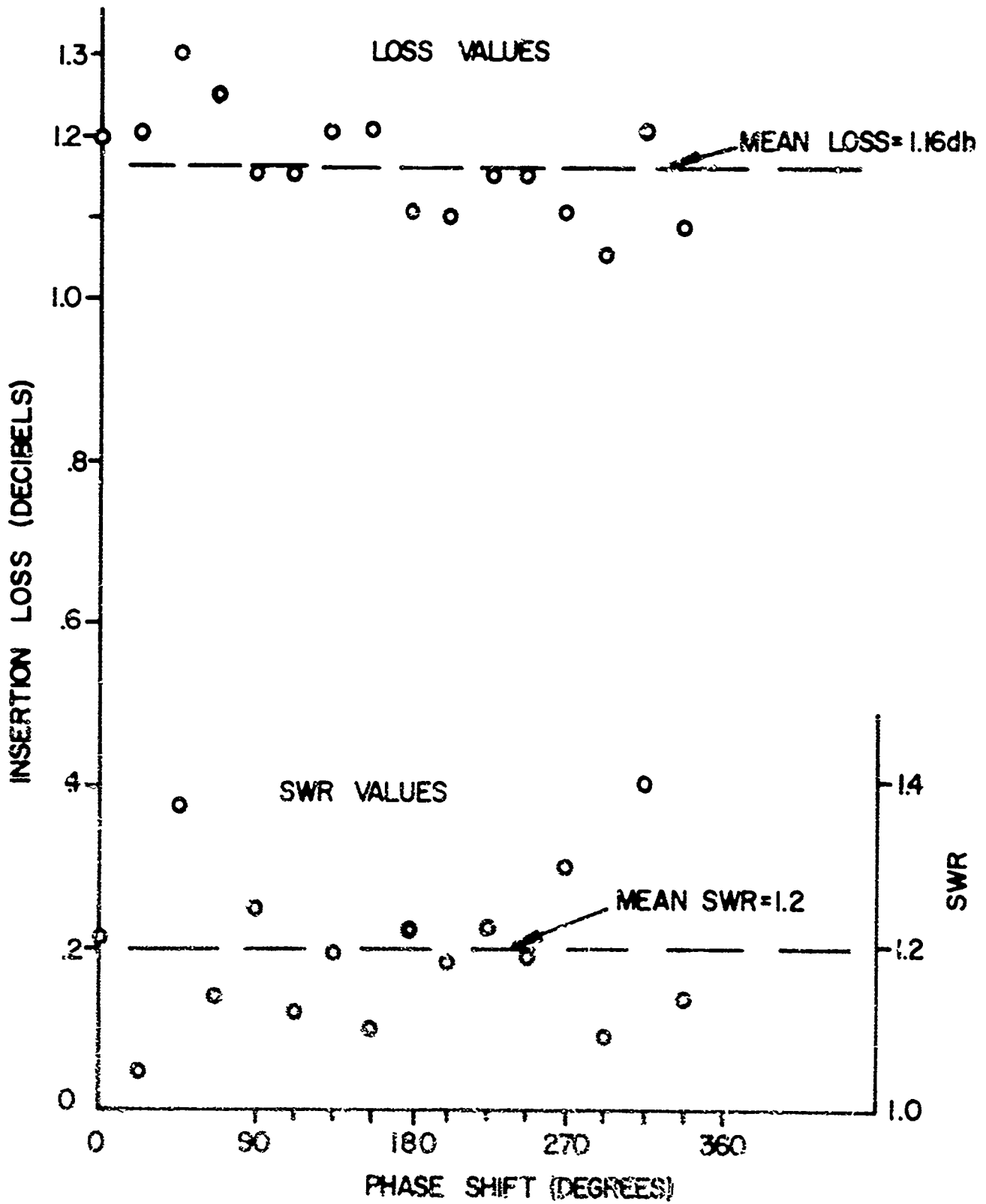
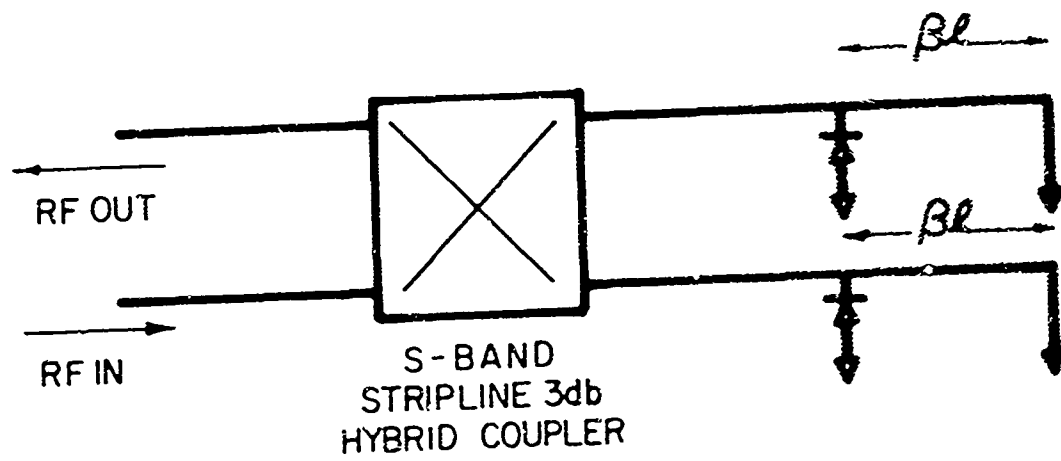


FIGURE 19



DIODES

DIODE	# 1	# 2
TYPE	PIN	PIN
BREAKDOWN VOLTAGE	2000V	2400V
CAPACITY AT ZERO BIAS	1.58 PF	1.81 PF
RESISTANCE AT 10 Ma	7.0 Ω	6.0 Ω
AT 50 Ma	1.9 Ω	2.0 Ω
AT 100 Ma	1.4 Ω	1.7 Ω

S BAND STEP PHASE SHIFTER EQUIVALENT CIRCUIT

FIGURE 20

FIGURE 21

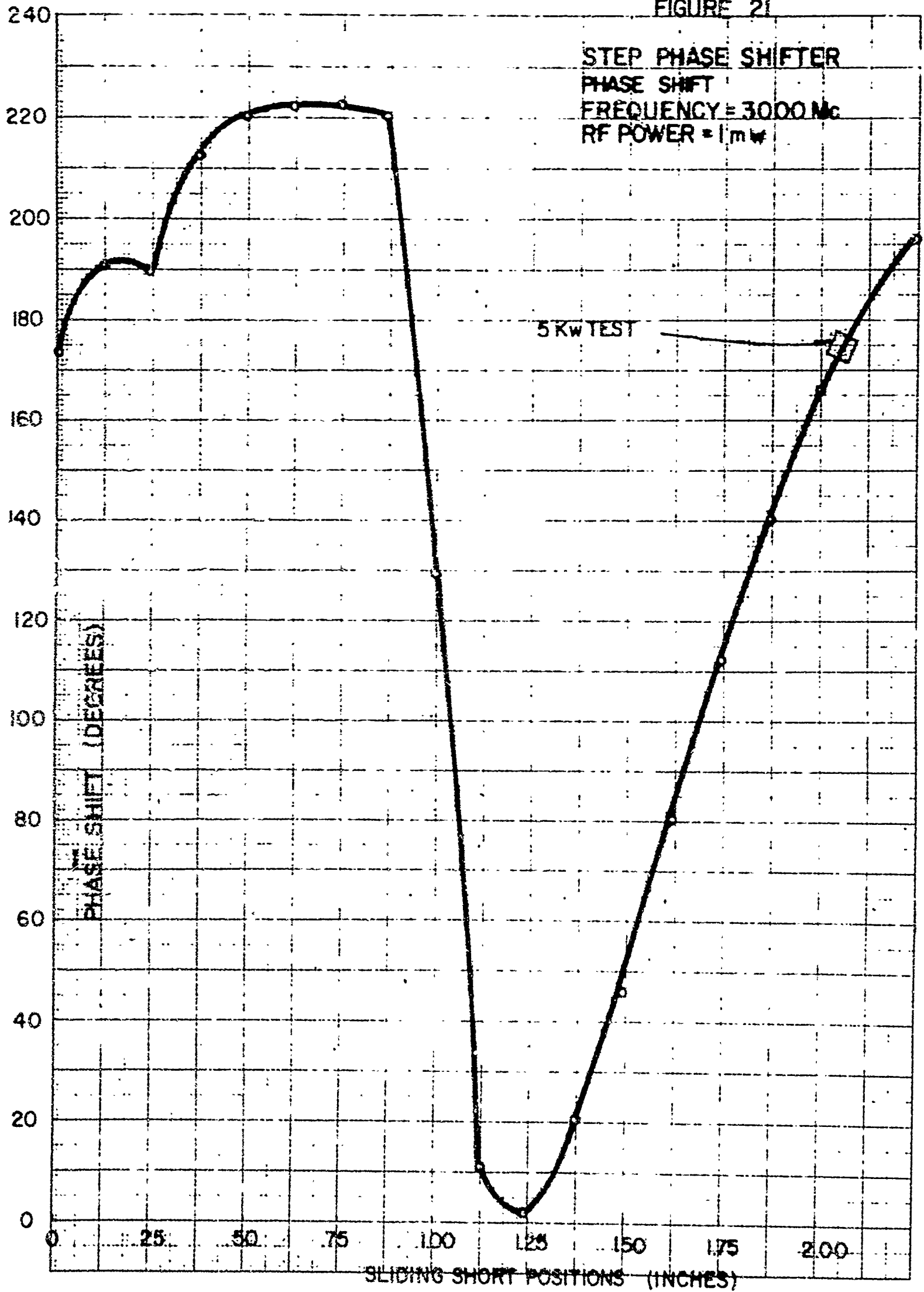
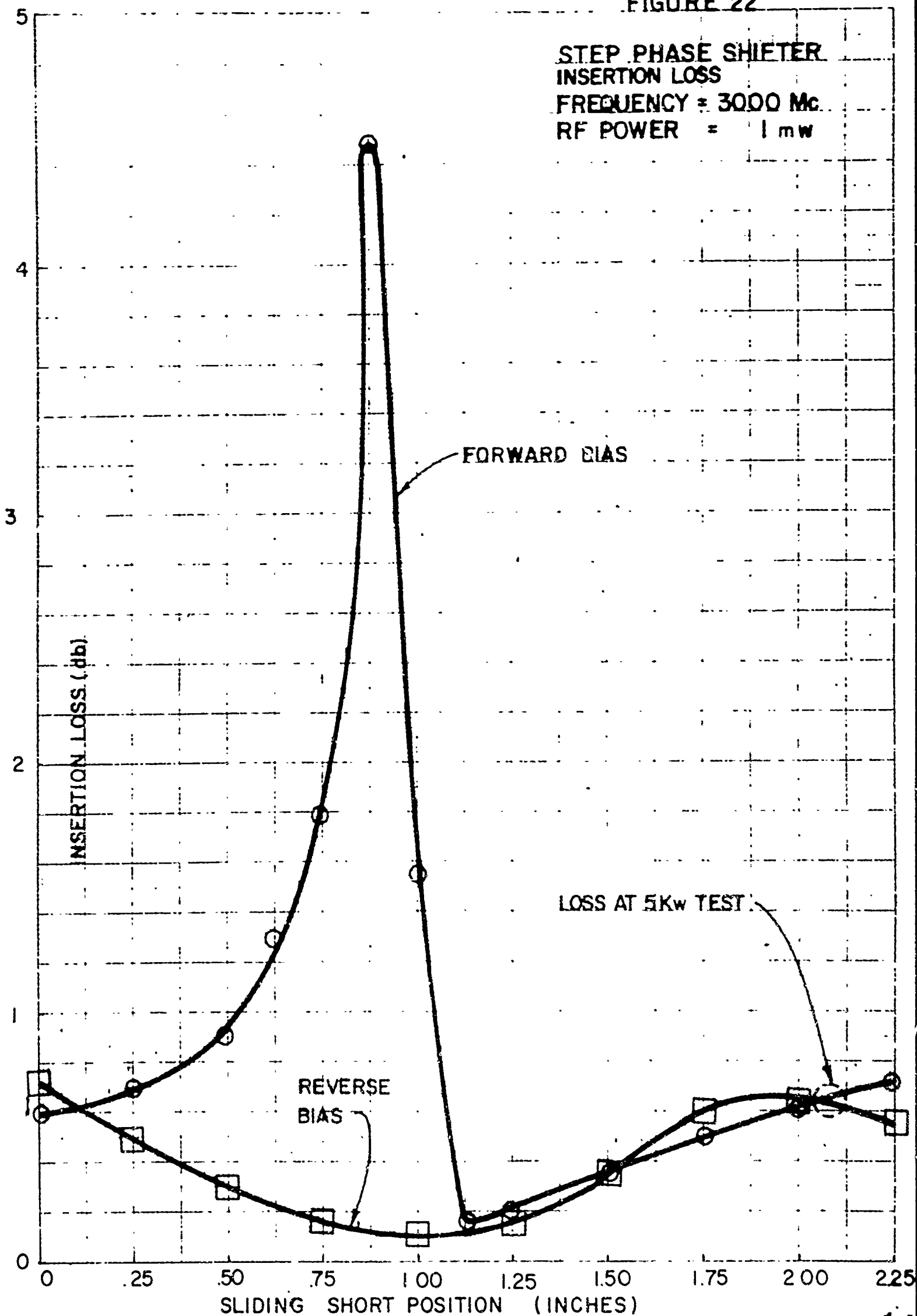


FIGURE 22



A maximum insertion loss in this range was 2.7 and the maximum sustainable RF power was found to be 5 kilowatts at the 180° phase shift -- worst -- condition. Further measurements were not made with this circuit because higher peak power capabilities with less total insertion loss were found achievable using a direct transmission circuit to be described in the next section.

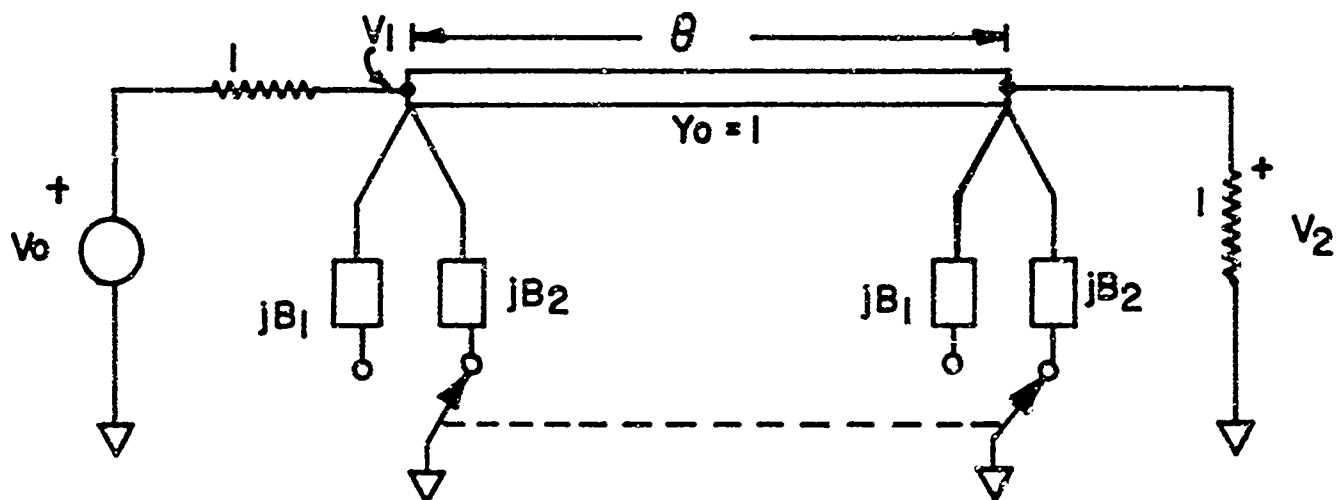
IV TRANSMISSION MODEA. DESIGN CONSIDERATION

1. Introductory Remarks: It was noted in the preceding section that highest power operation is accomplished by PIN diode circuits in which the phase shift contribution per diode is small, that is, when the diode offers only minimum perturbation to the transmission of the power. Therefore, it should be possible to design a circuit which approximates well the desired matched transmission property without need of a circulator or hybrid coupler. The equivalent form of such a circuit together with analytic expressions for phase shift is shown in Figure (23).

2. Phase Shift and Transmission Match Requirements

a. Equivalent Line Approximation: The exact expression for $\phi_{1,2}$ shown in Figure (23) reduces to the approximate form if the perturbations, $B_{1,2}$, are symmetrical, have small magnitude, and are spaced by about a quarter wavelength. Under these conditions, the prototype section is approximated by the equivalent line length of characteristic admittance Y_0' and electrical length, θ , as shown in Figure (24). This is particularly convenient for estimating the phase shift as well as the transmission match that can be obtained for a given set of circuit parameters.

b. Maximum VSWR: The maximum value of input VSWR to an arbitrary number of cascaded, identical, prototype sections terminated in a match load is given by Equation 3.



$$V_1 = V_2 A_0 e^{j\phi}$$

$$\phi_{1,2} = \cos^{-1} \left[\frac{\cos \theta - B_{1,2} \sin \theta}{\sqrt{1 - 2B_{1,2} \cos \theta \sin \theta + B_{1,2}^2 \sin^2 \theta}} \right]$$

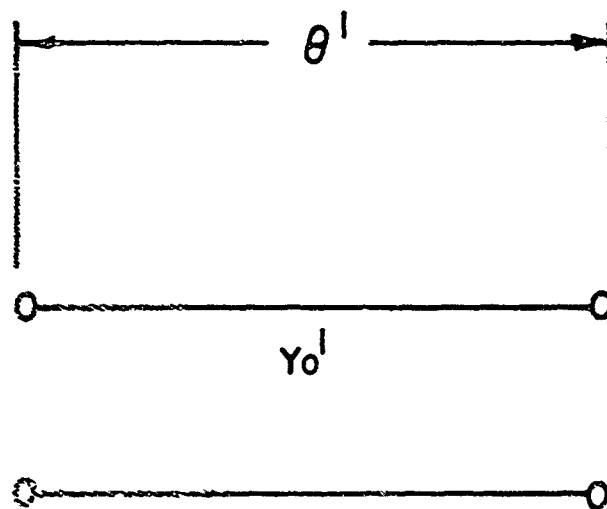
if $B_{1,2} \ll 1$
and, or, $\theta \approx \tan^{-1} \left(\frac{2}{B_{1,2}} \right)$

then $\phi_{1,2} \approx \cos^{-1} (\cos \theta - B_{1,2} \sin \theta)$

PHASE SHIFT = $\Delta \phi = \phi_1 - \phi_2$

FIGURE 23

TRANSMISSION PHASE SHIFTER



$$\theta^I = \cos^{-1}(\cos \theta - B_{1,2} \sin \theta)$$

$$\gamma_0^I = \sqrt{1 - B_{1,2}^2 + 2B_{1,2} \cot \theta}$$

FIGURE 24

EQUIVALENT LINE LENGTH APPROXIMATION

$$VSWR_M = \left(\frac{Y'_0}{Y_0} \right)^2 ; Y'_0 > Y_0$$

$$VSWR_M = \left(\frac{Y_0}{Y'_0} \right)^2 ; Y_0 > Y'_0$$

Equation (3)

c. Approximate Expressions: Insight into the phase shift to be obtained from a pair of switched susceptances, $B_{1,2}$, may be obtained by considering the geometric representation of Figure (25) which shows in vector form the approximate relationship for θ' . From this, it may be seen that the electrical length perturbation effected by switching the susceptance pair from the value B_1 to the value B_2 is equal approximately to the difference in the susceptances. Recognizably, this approximation is obtained from the previous approximation of Figure (23), and hence, is of second order. It is, however, quite appropriate for design purposes.

For example, if two susceptance values, $B_{1,2}$, are separated by about a quarter wavelength and have the values $\pm j 0.2$ respectively, the phase shift to be expected using the approximate expression is 0.4 radians or 22.9° . The approximation improves as θ approaches 90° , but even if θ is only 80° , with the same choice of switched susceptances, the exact expression indicates a phase shift of 21.6° would be obtained and demonstrates reasonable agreement with the approximate expression's result.

The maximum input VSWR to the match terminated cascade of an arbitrary number of similar such sections all switched to B_1 or

FIGURE 25



$$\sin \Delta \theta_2 = \frac{Z_0 B_2 \sin \theta + (1 - \cos \Delta \theta_2) \cot \theta}{\sin \theta} \approx Z_0 B_2$$

then

$$\Delta \theta_T \approx Z_0 |B_1 - B_2|$$

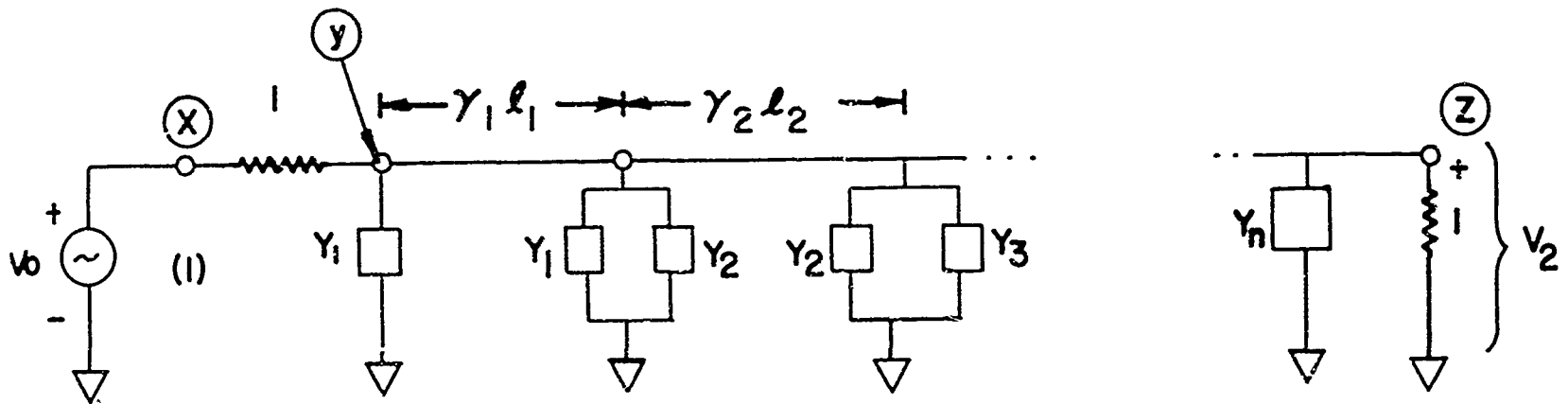
B_2 is calculated using Equation (3). The worst value, occurring when $B = -0.2$ and $\theta = 80^\circ$, is 1.09.

d. Exact Solution for Cascade Circuit: In practice, the cascade combination of a number of prototype sections, as shown in Figure (26), could serve to control a phased array antenna element. In this case, the phase shift -- or change in voltage phase between input and output ports -- of a particular prototype section in the cascade is not independent of the parameters of the other sections of the cascade, unless the transmission match of all sections is perfect. Reasonable approximation can be obtained with an economy of analytic labor by making the assumption that it is.

If computer facilities are available, however, an exact solution for the insertion loss and phase characteristic of the cascade may be made using the expressions of Figure (26). In this general case, it is assumed that the sections are not identical and that both line losses and control element losses are significant.

The phase shift through such a cascade may be calculated using the gain expression for any particular combination of Y_j 's and $(\gamma l)_j$'s. The phase shift to be obtained for any such state then may be estimated by taking the difference in the angle of the gain expression calculated for the different parameter combinations. Similarly, an exact value of insertion loss also may be calculated.

e. Approximate Loss Calculations: Small perturbation theory also can be used to estimate the insertion loss of a transmission



$$\begin{bmatrix} a & b \\ c & d \end{bmatrix}_{yz} = \prod_{j=1}^n \begin{bmatrix} \cosh(\gamma_j \ell_j)^I & Z_c^I \sinh(\gamma_j \ell_j)^I \\ Y_c^I \sinh(\gamma_j \ell_j)^I & \cosh(\gamma_j \ell_j)^I \end{bmatrix}$$

where $(\gamma_j \ell_j)^I = \cosh^{-1} (\cosh \gamma_j \ell_j + Y_j \sinh \gamma_j \ell_j)$

and $Y_c^I = \frac{1}{Z_c^I} = \left[1 + 2Y_j \coth \gamma_j \ell_j + Y_j^2 \right]^{1/2}$

$$\begin{bmatrix} A & B \\ C & D \end{bmatrix}_{xz} = \begin{bmatrix} 1 & 1 \\ 0 & 1 \end{bmatrix} \cdot \begin{bmatrix} a & b \\ c & d \end{bmatrix}_{yz}$$

$$V_0 = (A+B) V_2$$

FIGURE 26

EXACT GAIN EXPRESSION FOR GENERAL TRANSMISSION
PHASE SHIFTER CASCADE

phase shifter. Loss contributions are incurred from the conductive portion, G , of the shunting admittance, Y , as well as the real component of the complex propagation constant, $\gamma = \alpha + j\beta$. Since the shunt admittances, Y , are assumed small perturbations compared to the line admittance, the loss incurred by them is approximately equal to the normalized conductance, G . Then if this total is added to the line losses which would be measured with all shunt admittances removed, the resulting total is an approximation of the phase shifter insertion loss.

For example, if a single prototype, match terminated section consists of two normalized admittances, $Y = 0.02 - j 0.2$, which are spaced by 90° and if the transmission line loss is approximately 0.1 decibel per wavelength, then the insertion loss for the section is estimated to be 0.202 decibels. The exact expression for insertion loss in this case may be obtained from Figure (15) and is shown below as Equation (4).

$$I.L. = \frac{1}{4} \left| 2(1 + Y) \cosh \gamma l + (2 + 2Y + Y^2) \sinh \gamma l \right|^2$$

Equation (4)

From this expression, the exact insertion loss is calculated to be 0.204 decibels, if the spacing were decreased to 80° , then the exact loss becomes 0.221 decibels. The approximation improves with the transmission match.

The loss parameters here are higher than those of the circuits to be discussed and thus the approximation is useful even for several cascaded sections.

B. CIRCUIT IMPLEMENTATION

1. L-Band Frequency Range

a. Stub Approach to Implement $jB_{1,2}$: At L-band frequencies, the impedance values under forward and reverse bias conditions for a PIN diode approach short and open circuits when compared to 50 ohm coaxial line impedance. A means for effecting switched susceptance values, $jB_{1,2}$, using the PIN diodes is diagrammed in Figure (27). In essence, the diode changes electrical length of the short circuited stub pairs which are, in turn, shunt mounted in the main transmission path. The estimated parameters described by Figure (27) are given below in Table 1.

TABLE 1

R_F	0.6 ohms
R_R	2 ohms (estimated)
C_j	0.6 picofarads
C_p	0.3 picofarads
L	1 nanohenry
$Z_o = Z_s$	50 ohms

An experimental model was constructed in which the average stub length $(\theta_1 - \theta_2)/2$ was made equal to nearly a quarter wavelength. In this way, the change in switched susceptances is approximately equal to the difference $\theta_2 - \theta_1$; and, accordingly, the phase shift obtained is approximately equal to this difference.

- ① FORWARD BIAS
② REVERSE BIAS

FIGURE 27

L-BAND TRANSMISSION PHASE SHIFTER PROTOTYPE

b. Measured Transmission and Reflection Parameters:

Eight such identical pairs of switched line lengths were mounted across a 50 ohm coaxial circuit, shown pictorially in Figure (28). The measured phase shift and insertion loss as functions of the number of reverse biased diode pairs are plotted in Figures (29) and (30) respectively. The sections were adjusted so as to be mechanically similar to one another once the dimensions required to produce about $1/16$ of a wavelength phase shift per section were established. The resulting average phase shift per section was 23.0° for the total range of 0° to 184° in eight equal steps. The increase in electrical length of the phase shifter, as succeeding sections were reverse biased, was measured. The steps varied between 21° and 24° . Thus, close electrical similarity was achieved even though the sections were made only mechanically similar.

The insertion loss shown in Figure (30) has a maximum value of 0.7 db with all diodes forward biased and a minimum value of 0.35 db with all reverse biased. Under forward biased conditions, a diode loss of only about 0.3 db total would be expected from the equivalent circuit assumed. The circuit losses are also nearly of this magnitude. The reverse biased equivalent circuit assumed for the diode would be expected to cause an aggregate diode loss of less than 0.1 decibel. Thus, the measured change of about 0.3 db of insertion loss is reasonable. Equal loss for all bias states should be obtainable by choosing a higher characteristic impedance for the stubs. In this way, the insertion loss under reverse bias would be increased and that under

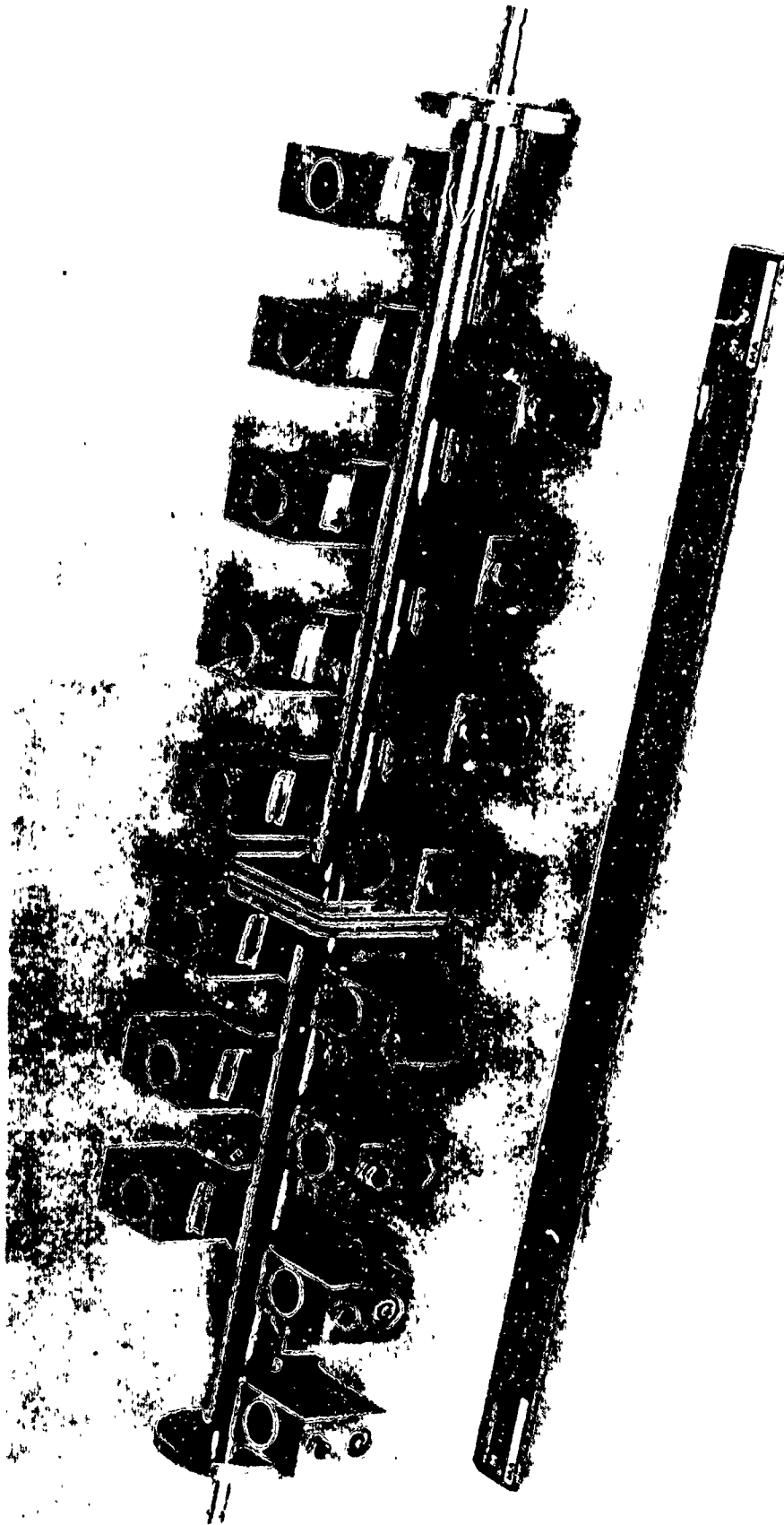


FIGURE 28
PHOTOGRAPH OF L-BAND TRANSMISSION PHASE SHIFTER

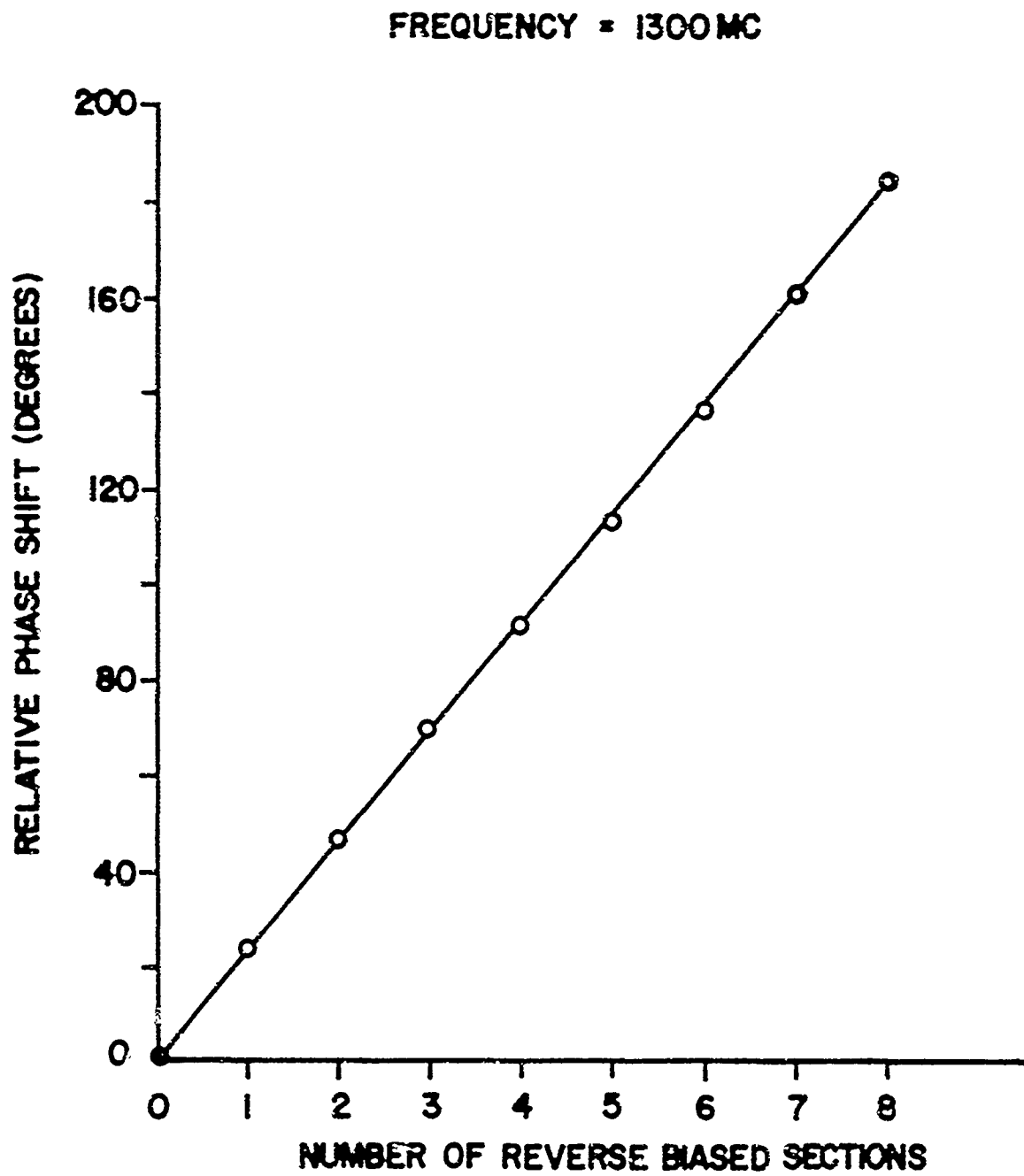


FIGURE 29

MEASURED PHASE SHIFT OF L-BAND MODEL

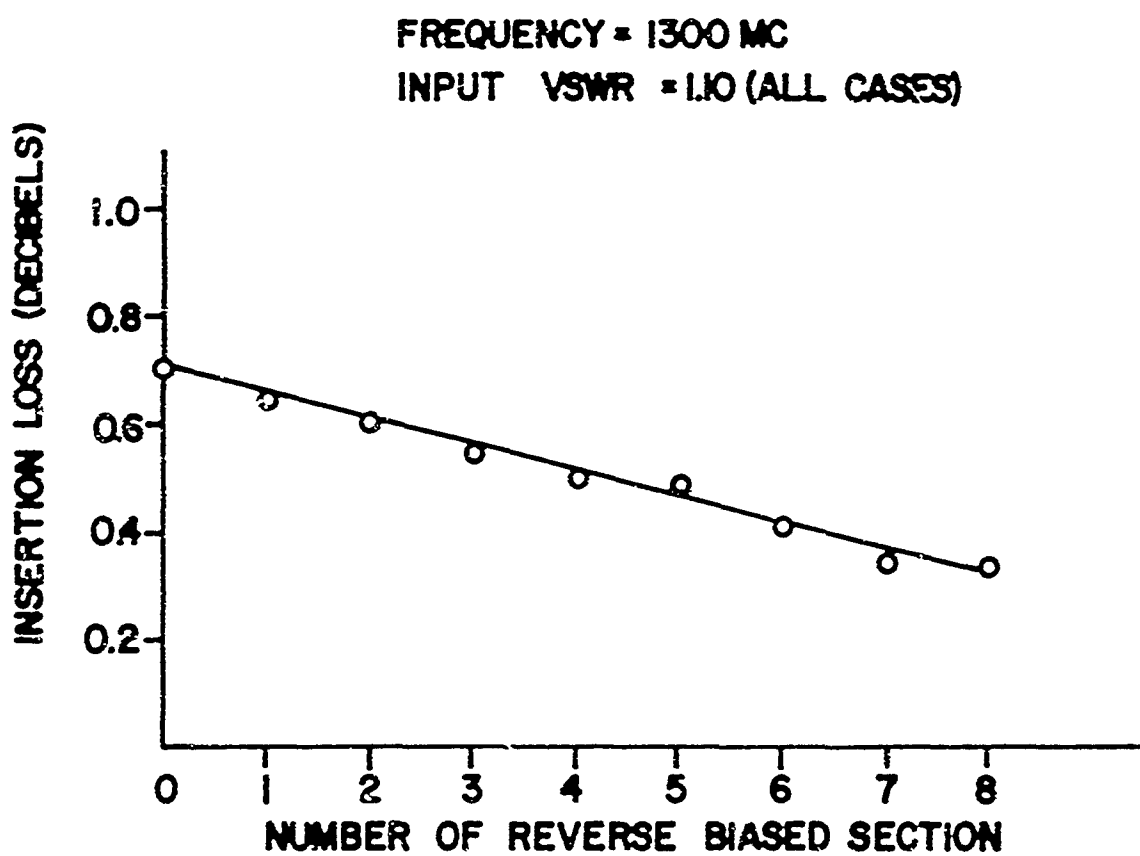


FIGURE 30

MEASURED INSERTION LOSS OF L-BAND MODEL

forward bias could be decreased. A value of approximately 0.4 db or less should be achievable. The voltage limited peak power capability, however, would be reduced.

c. Maximum Power Capability: When the diodes are forward biased, the maximum power of operation is determined from a consideration of the insertion loss, diode heat dissipating capacity, duty cycle of operation and pulse length. In this circuit, each diode dissipates when forward biased approximately 1% of the power incident, and is capable of dissipating about 10 watts continuously. Thus, a 1 kilowatt continuous wave power level could be sustained. For short pulses, the maximum power dissipated in a diode may be determined conservatively by assuming that no cooling takes place during the pulse. Consideration of the geometry of the silicon wafer of which the diodes were fabricated indicates the heat sinking capacity is approximately 50 (watt) x (microseconds) per degree Centigrade of temperature rise. Maximum temperature increase is related to the ambient. Typically for silicon welded type diodes, a 100°C. change within the pulse often may be tolerated, hence the experimental circuit could be expected to sustain 500,000 watt-microsecond RF pulsed power under forward bias. However, as was noted in Section III, operation at high peak power of the phase shifter also is limited by the maximum RF voltage which may be impressed across the diodes under reverse bias. Since the reverse biased diode represents a very high impedance, and since the length of the short circuit stub is approximately a quarter wavelength, the voltage appearing across the diode, V_D , is

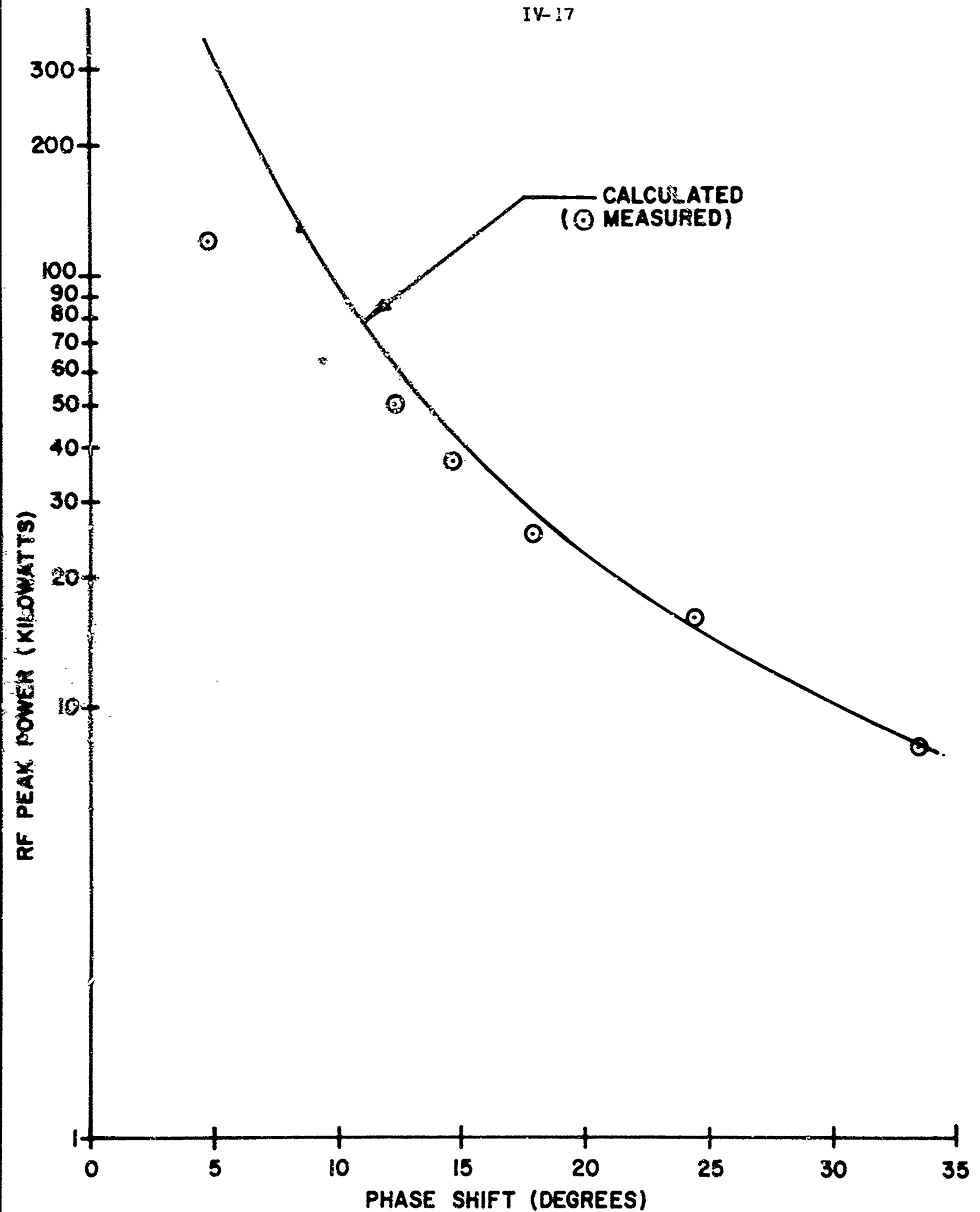
given approximately by Equation (5).

$$V_D \approx V_L \sin (\theta_2 - \theta_1), \quad \text{Equation (5)}$$

For any particular maximum sustainable RF voltage, V , the peak power, P_m , is given by Equation (6).

$$P_m \approx \frac{V_M^2}{Z_o \sin^2 \Delta \theta} \quad \text{Equation (6)}$$

From this, it is seen that the voltage limited peak power capability increases inversely as the square of the phase shift obtained. This was examined experimentally by determining the maximum power of operation for a phase shifter yielding about 33° of phase shift and comparing this to the maximum level sustainable for lesser values of phase shift using the same diodes. Two 800 volt breakdown PIN switching diodes were employed and the maximum power levels were defined to be those at which the diodes' leakage current increased by 5 microamperes from the 100 volt bias supply. Typically, an increase in the reverse bias current of this magnitude precedes catastrophic failure of the diodes. (These tests were performed at an RF frequency of 1300 megacycles and an operating pulse length and duty cycle of 5 microseconds and 0.001 respectively.) The measured results can be seen compared with those calculated for phase shift values as small as 5° in Figure (31). Operation to approximately 120 kilowatts was sustained with a value of 5° phase shift prevailing. More phase shift was anticipated for this power. Discrepancies may be due to the inadequacy of the equivalent circuit model to describe this small phase shift case; accuracy of the model will now be discussed. Subsequent testing of the 8-section model yielded 140 KW peak power capability with 5° phase shift per section.



PHASE SHIFT VS PEAK POWER OBTAINED
WITH TRANSMISSION CIRCUIT USING TWO
800 V SWITCHING DIODES
FIGURE 31

d. Variation of Phase Shift with Frequency: A combination of several factors influences the phase shift versus frequency characteristic.

1. The difference $\theta_2 - \theta_1$ increases with frequency and with it the phase shift.

2. With increasing or decreasing frequency, the average value $(\theta_2 - \theta_1)/2$ departs from 90° and then $\theta_2 - \theta_1$, increases due to the cotangent expression, $B_{1,2} = \cot \theta_{1,2}$.

3. Only approximately does the diode switch between short and open circuits, see Figure (27), under forward bias, package inductance and bypass capacity by design are series resonant at the center frequency. At reverse bias, the diode represents a capacity of about 0.8 pf.

4. The line length behind the diode was terminated by a spring finger type, sliding short. The impedance of this section and the electrical length are known only approximately. Greater error would be experienced for the smaller values of $\theta_2 - \theta_1$. (This was where largest departures from calculated performance were measured in high power tests.)

However, it was found that fair approximation can be achieved even with only considerations (1) and (2). For example, the measured phase shift versus frequency, as shown plotted in Figure (32), was graphed and the frequency at which the derivative of phase shift versus frequency was equal to unity was used as a measure of the center

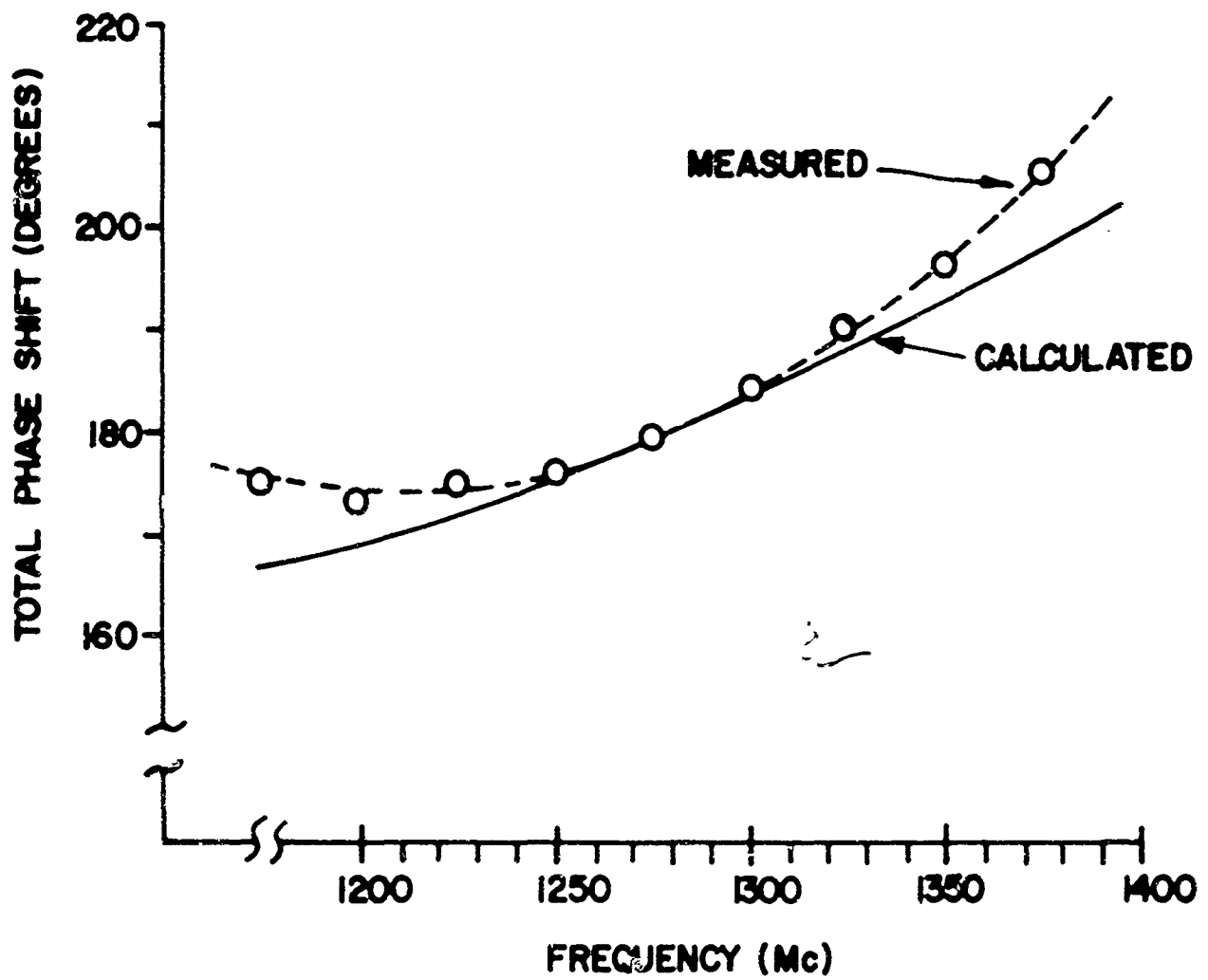


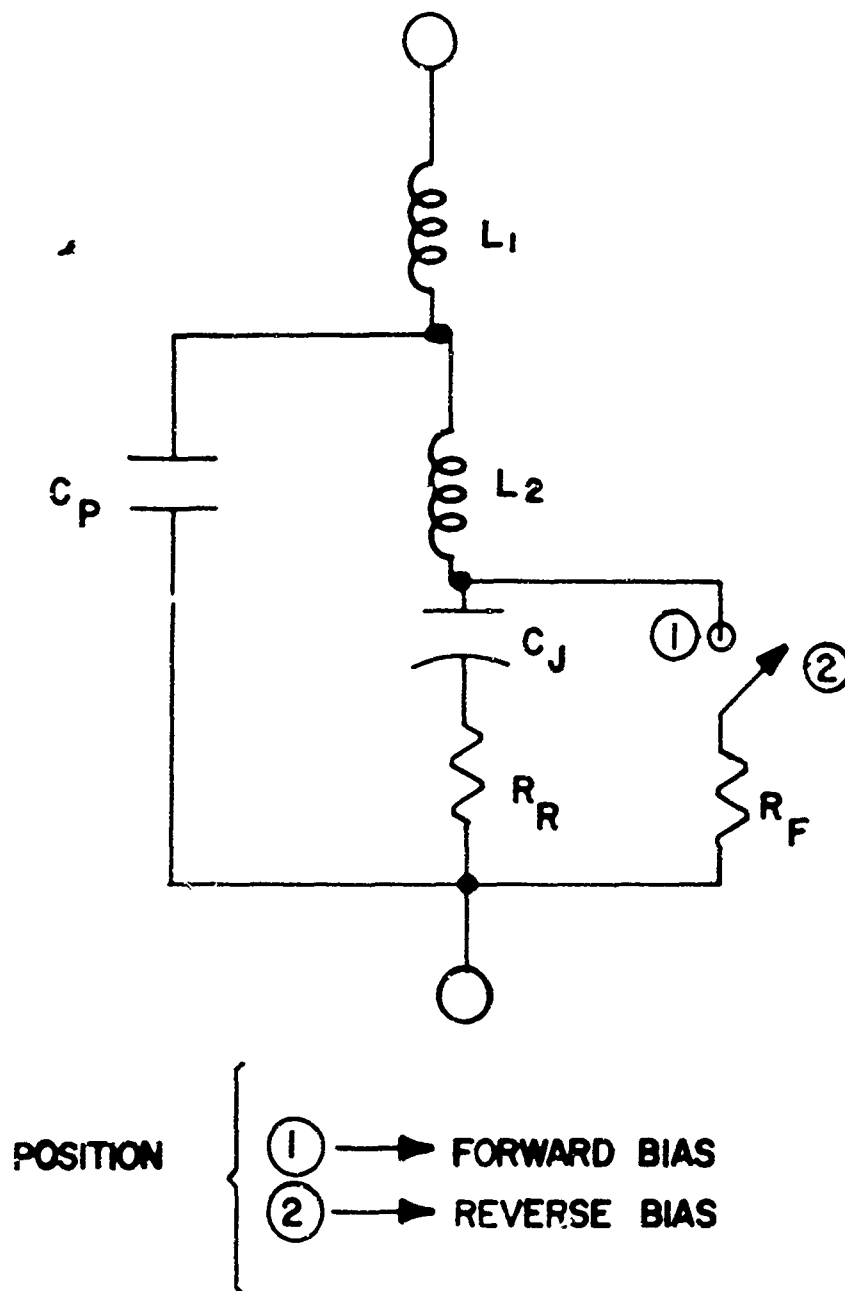
FIGURE 32

CALCULATED AND MEASURED PHASE
SHIFT VERSUS FREQUENCY

frequency of the device. This occurred at about 1260 Mc. Assuming this frequency to be that at which the average value of θ , $(\theta_2 - \theta_1)/2$, was equal to one quarter wavelength, the frequency variation of phase shift was plotted using points (1) and (2). These calculated results are shown in Figure (32) and are seen to agree with the measured performance to within 1% over a 90 Mc, or 7% frequency band. This is, for many practical operating radars, the full system bandwidth; and thus, the approximation seems quite useful for design purposes.

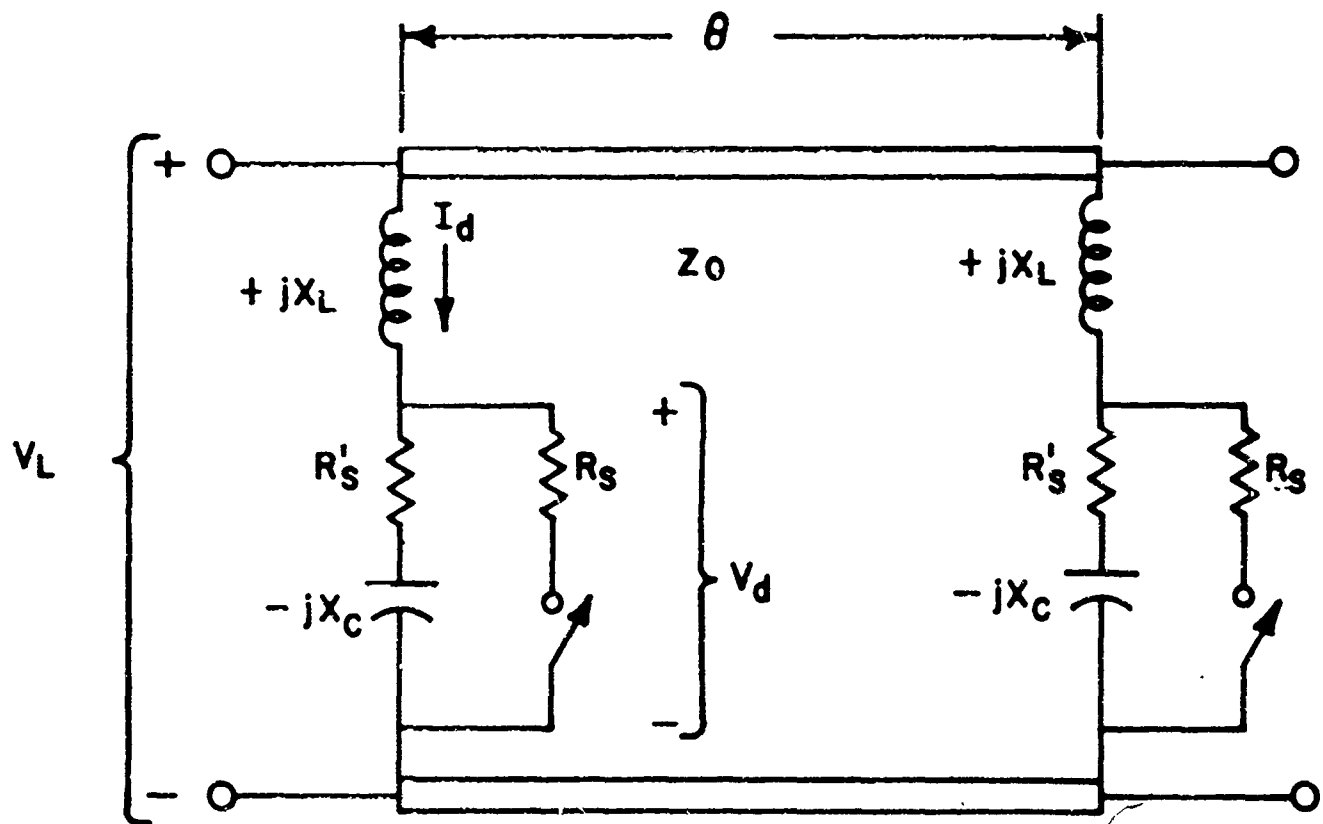
IV B. 2. S-Band Circuit

a. Diode Reactance Circuit: At S-band frequencies, reactive circuit values associated with the PIN diode and its package may not be neglected as was done at L-band. These reactances are often considered parasitic values particularly in switch designs where their effect is to limit usable bandwidth. A complete equivalent circuit for the PIN diode and its two biased states is shown in Figure (33). If the inductance L_2 is assumed small compared to L_1 , then the package capacity, C_p , may be considered lumped together with the junction capacity C_j . Typical values of the total inductance and capacity are 1 nanohenry and 0.8 picofarads respectively. At 3000 Mc, then, the diode varies essentially between a capacitive reactance at reverse bias and an inductive reactance at forward bias. If additional inductance is added in series with the diode package and the resultant circuit placed in shunt with a transmission line, a switchable susceptance of constant magnitude with variable polarity, $\pm jB_{1,2}$, is achieved. This is implemented at 3000 Mc by an inductance



PIN DIODE EQUIVALENT CIRCUIT

FIGURE 33



EQUIVALENT CIRCUIT, WITH LOSS, OF
ITERATIVELY LOADED LINE PHASE
SHIFTER PROTOTYPE NETWORK
FIGURE 34

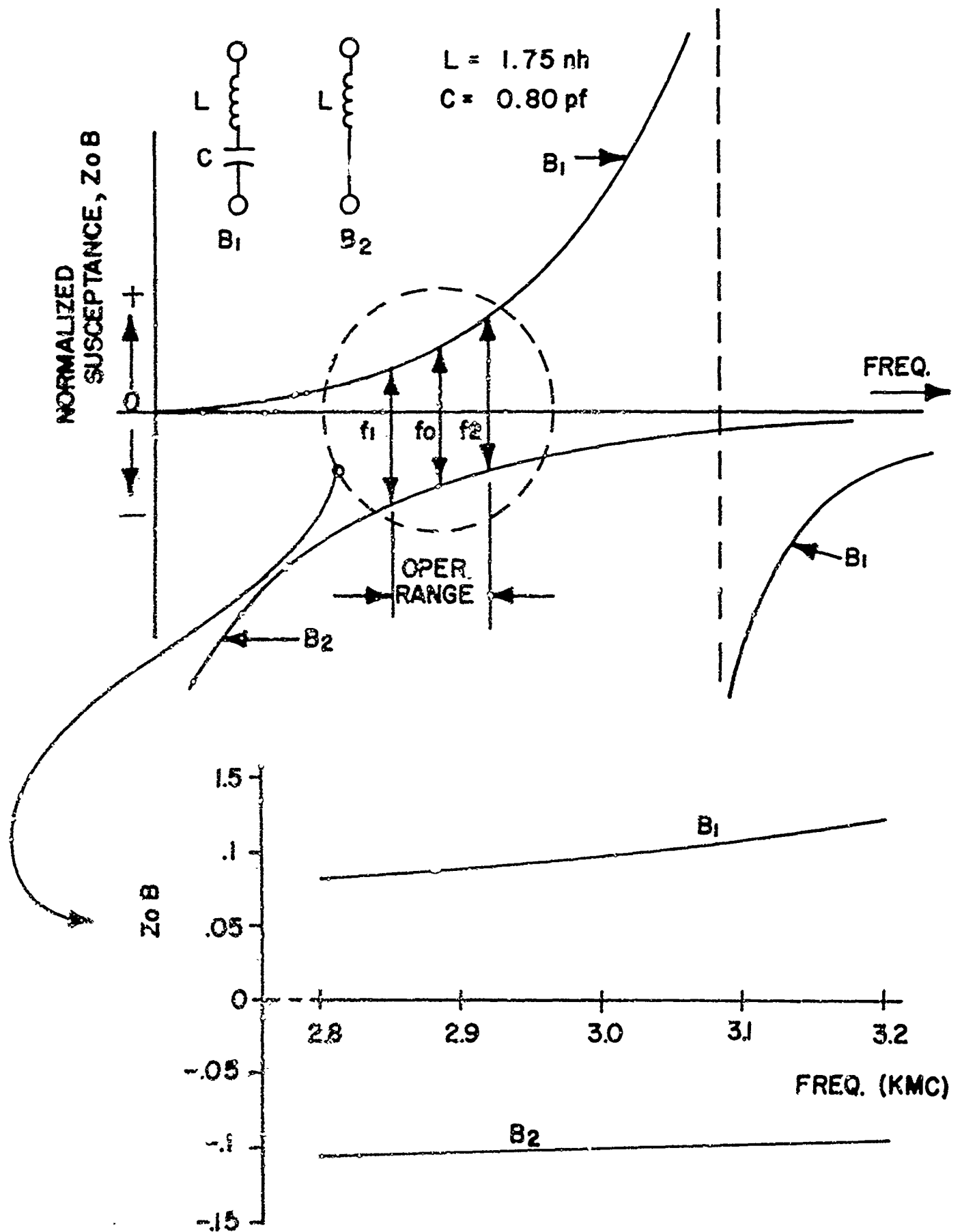
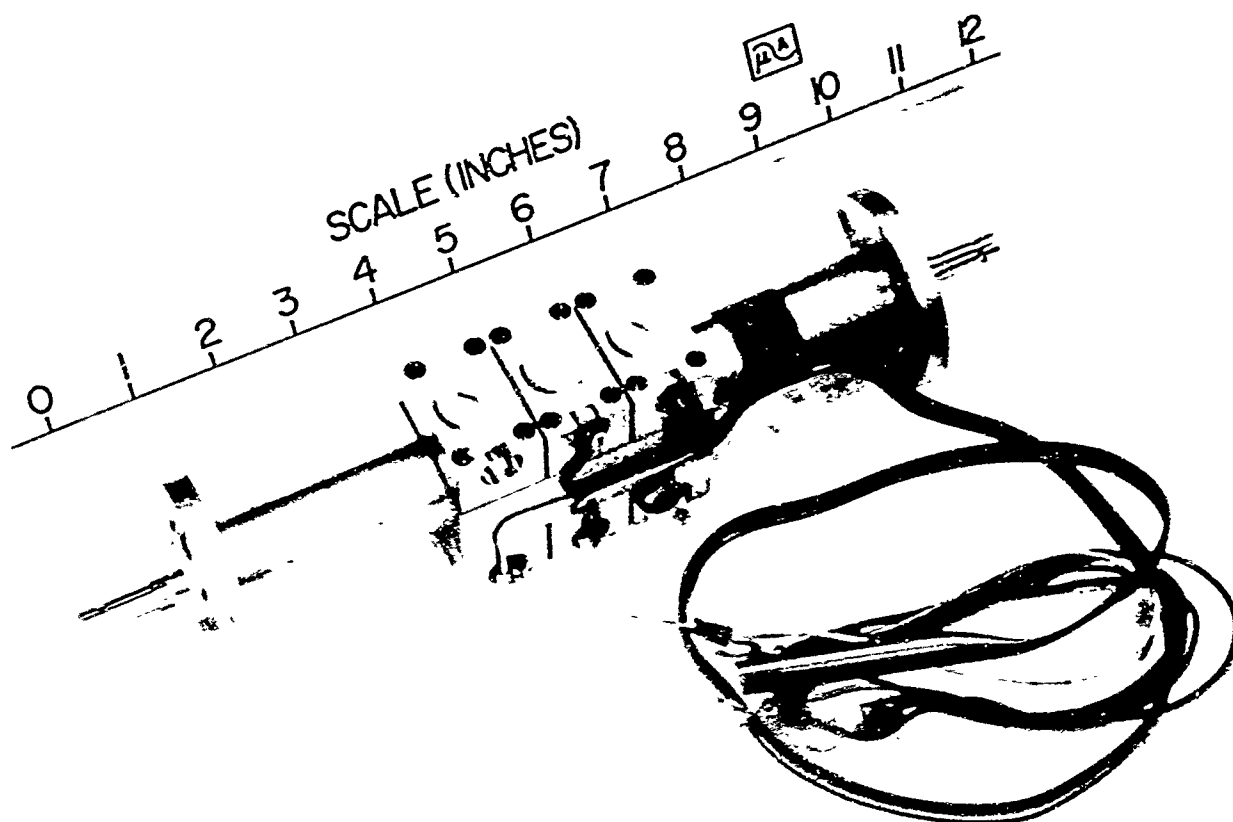
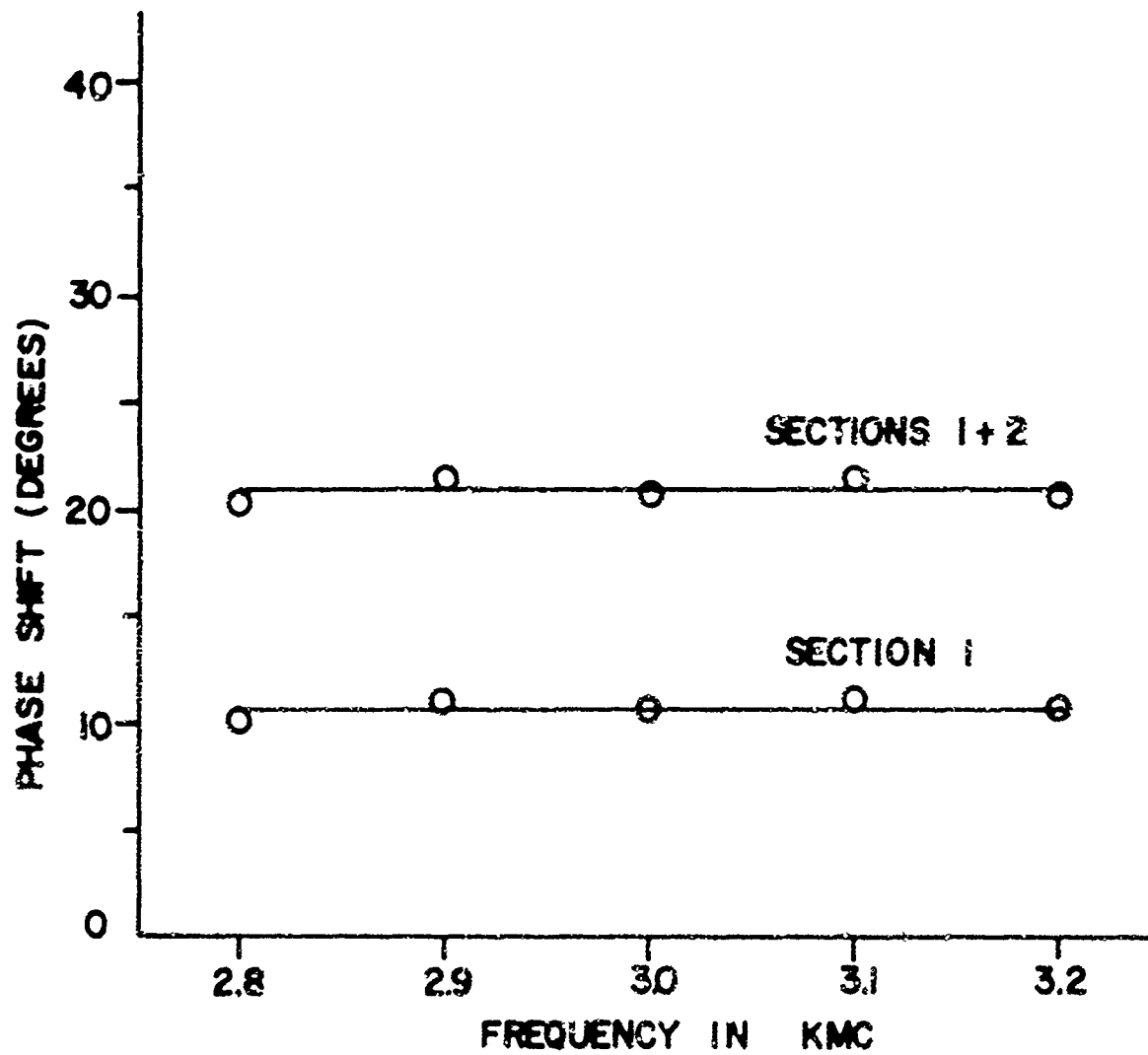


FIGURE 35

SUSCEPTANCE VS. FREQUENCY DIAGRAM

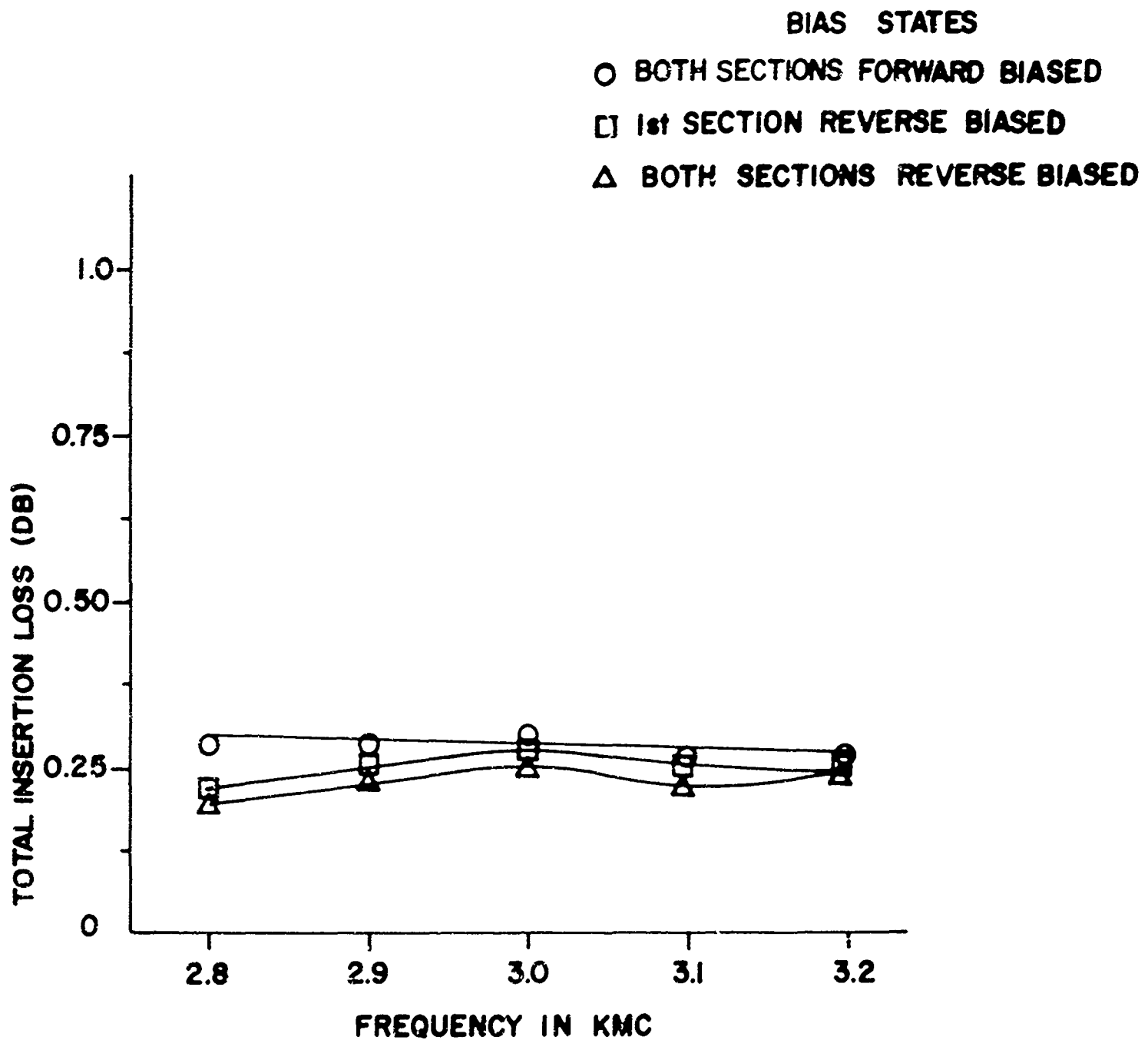


PHOTOGRAPH OF TWO SECTION TRANSMISSION PHASE
SHIFTER



PHASE SHIFT CHARACTERISTIC OF TWO SECTION
TRANSMISSION PHASE SHIFTER

FIGURE 37

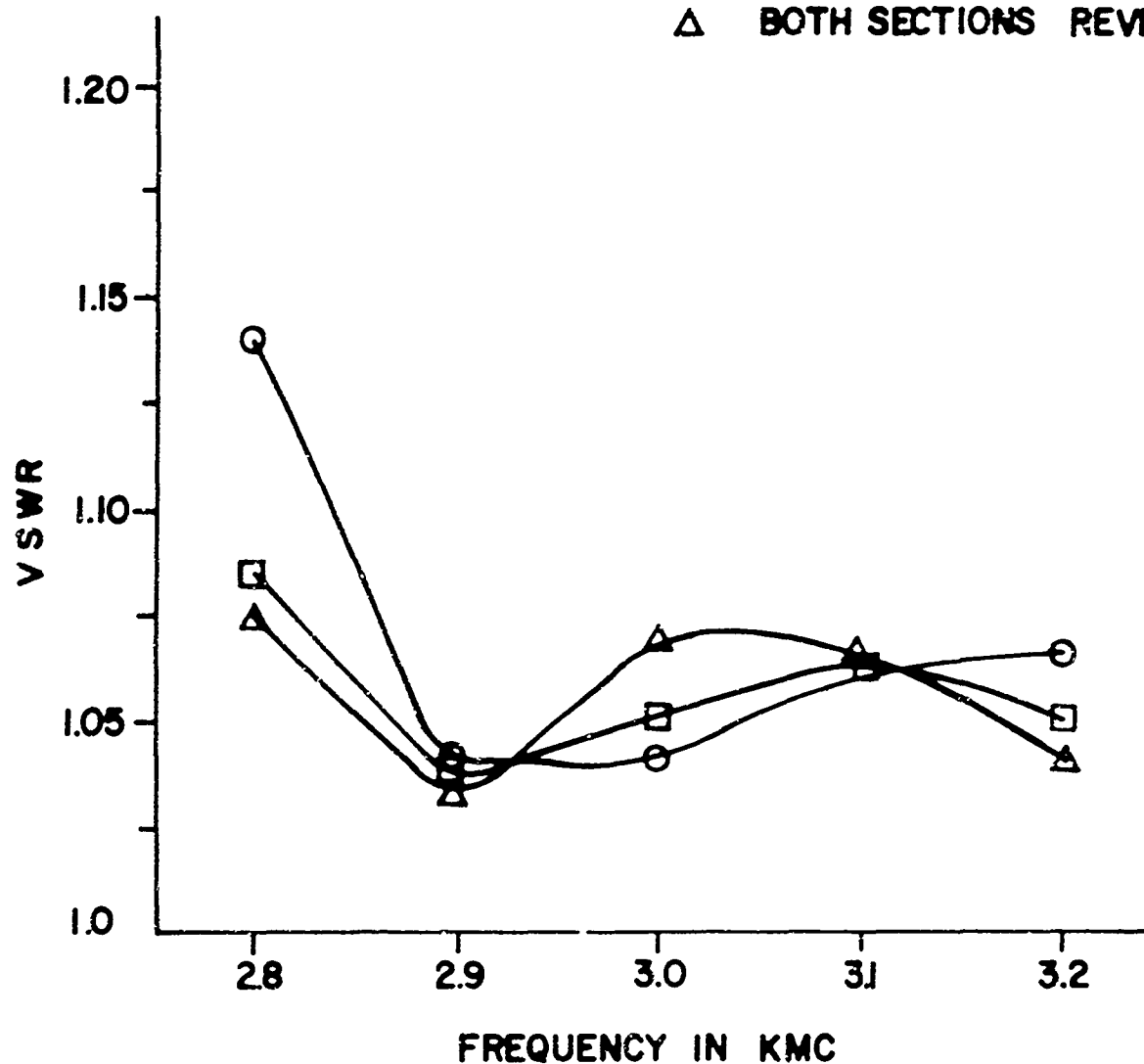


**INSERTION LOSS CHARACTERISTIC OF TWO SECTION
TRANSMISSION PHASE SHIFTER**

FIGURE 38

BIAS STATES

- BOTH SECTIONS FORWARD BIASED
- 1st SECTION REVERSE BIASED
- △ BOTH SECTIONS REVERSE BIASED



VSWR CHARACTERISTIC OF TWO SECTION
TRANSMISSION PHASE SHIFTER

FIGURE 39

of about 1.8 nanohenries and the capacitance of 0.8 picofarads. An equivalent circuit of a prototype section of this phase shifter may be seen in Figure (34).

b. Small Variation of Phase Shift with Frequency: Interestingly, this circuit implementation of switch susceptances yields a difference value, $B_2 - B_1$, which is nearly constant with frequency. Reference to Figure (35) indicates why this is true. The line shunting susceptance, B_1 , resulting when the diode is reverse biased, increases with frequency to the point of series resonance, which is above the desired range of operation. The susceptance, B_2 , resulting from the line shunting inductance of the forward biased diode decreases with frequency and, over the particular range of values chosen for this model, the difference in these two values, also shown plotted in Figure (35), remains nearly constant with frequency.

c. Measured Performance of Experimental Models: The phase shift to be obtained from a pair of the switched susceptances described is proportional to the characteristic line impedance in which they are mounted provided that the magnitude of switched susceptance is small in comparison to the characteristic admittance of the transmission line. A two-section phase shifter using four similar diodes spaced in pairs by about a quarter wavelength was constructed as may be seen in the photograph of Figure (36). Measurements of phase shift, insertion loss and input VSWR made over the frequency range 2800 Mc to 3200 Mc are also shown in Figures (37), (38) and (39) respectively. The characteristic impedance

in the line section in which the diodes were mounted was 3.3 ohms. Broadband, three section, quarter wavelength, coaxial line transformers having a Tchebyscheff distribution of reflection coefficients at each end of the diode loaded section were used to transform this low impedance to the 50 ohm impedance of the measurement equipment.

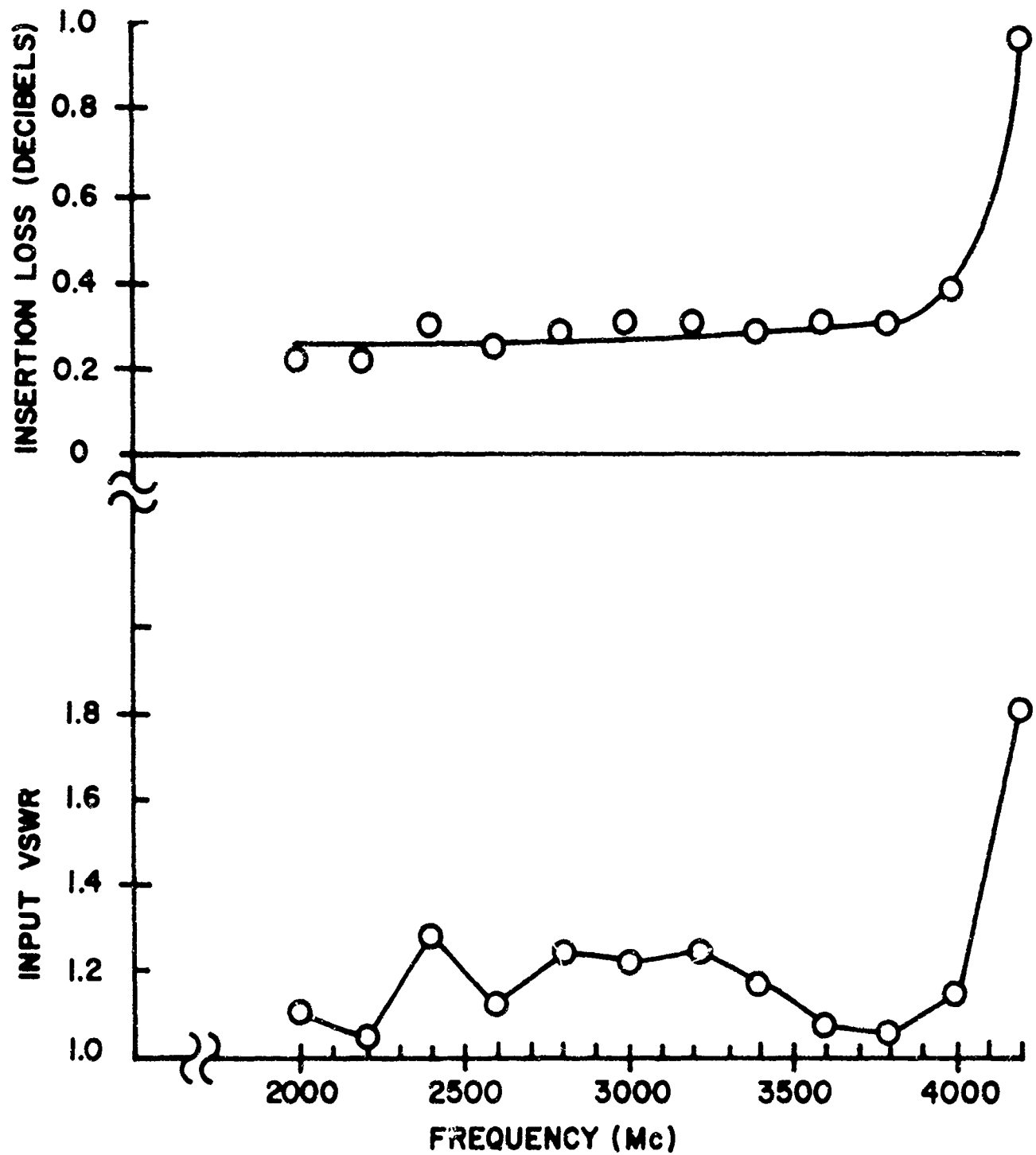
As may be seen from Figure (37), the phase shift was approximately equal to 11° per section. This was expected since the normalized switch susceptances are $\pm j 0.1$ for an estimated phase shift of 0.2 radians or about 11° . The measured insertion loss and VSWR of the transformer and phase shifter aggregate is seen to be less than 0.3 decibels and 1.18 over the 14% frequency band. The contributions to these values resulting from the transformer and low impedance line circuit with diodes removed were measured independently and found to be 0.25 decibels insertion loss and 1.10 maximum VSWR over the same frequency range. Thus, the diodes are seen to impart the desired phase shift function with minimal mismatch and insertion loss contributions to the circuit in which they are mounted.

A second experimental model was constructed using a transmission line impedance of 6.25 ohms and 16 diodes arranged in 8 pairs, again with quarter wavelength spacing at 3000 Mc. The photograph of this model is shown in Figure (40). The insertion loss and input VSWR of this circuit measured with the diodes removed is as shown in Figure (41). From this, it is seen that increasing the length of the low impedance section does not appreciably increase the insertion loss or input VSWR. Thus, a

BLANK PAGE



FIGURE 40
PHOTOGRAPH OF S-BAND TRANSMISSION PHASE SHIFTER



PERFORMANCE OF S-BAND 8 SECTION ITERATIVE PHASE
SHIFTER WITH DIODES REMOVED
FIGURE 41

multi-section phase shifter circuit is even more efficient in that lesser insertion loss per phase shift section results as the total number of sections is increased.

The same values of capacity and inductance are associated with the diode and its mount as applied for the 3.3 ohm model; these are 0.8 picofarads and 1.8 nanohenries. Since the characteristic impedance of the transmission line, however, was twice the value of that used previously, about 22° of phase shift per section would be expected. Indeed, this is verified by the measured characteristic shown in Figure (42). Again, a small variation of phase shift obtained for various frequencies is exhibited. In this case, the total variation in phase shift obtained over the 14% frequency bandwidth from 2800 Mc to 3200 Mc is only about $4\frac{1}{2}\%$. Some of this variation may have occurred due to the variations in parameters of the individual diodes used. Typical variations of the diode capacity values were ± 0.1 picofarads. Direct measurement of the mount and diode package series inductance is not estimable accurately, since the diodes represent only small perturbations to the transmission line. All mounts were adjusted so as to be mechanically similar and thus, variations of the mount inductance as well as the diode package inductances are assumed to be small.

The maximum value of input VSWR to this 8-section phase shifter was 1.3 for all of the bias states examined. As seen from Figure (42), the maximum value of insertion loss was approximately 0.9 decibels and the minimum value of 0.6 decibels. Approximately 0.3 decibels

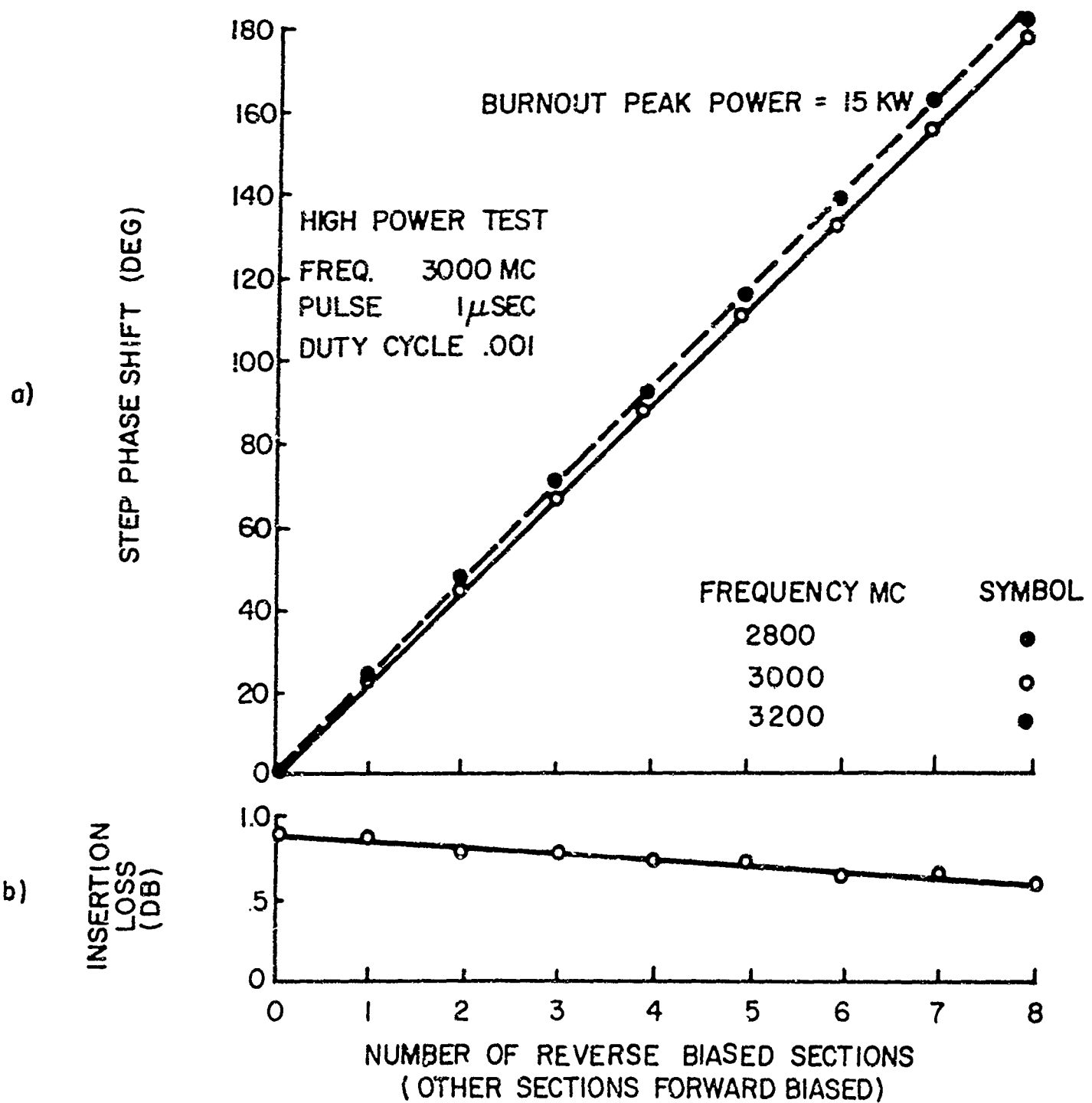
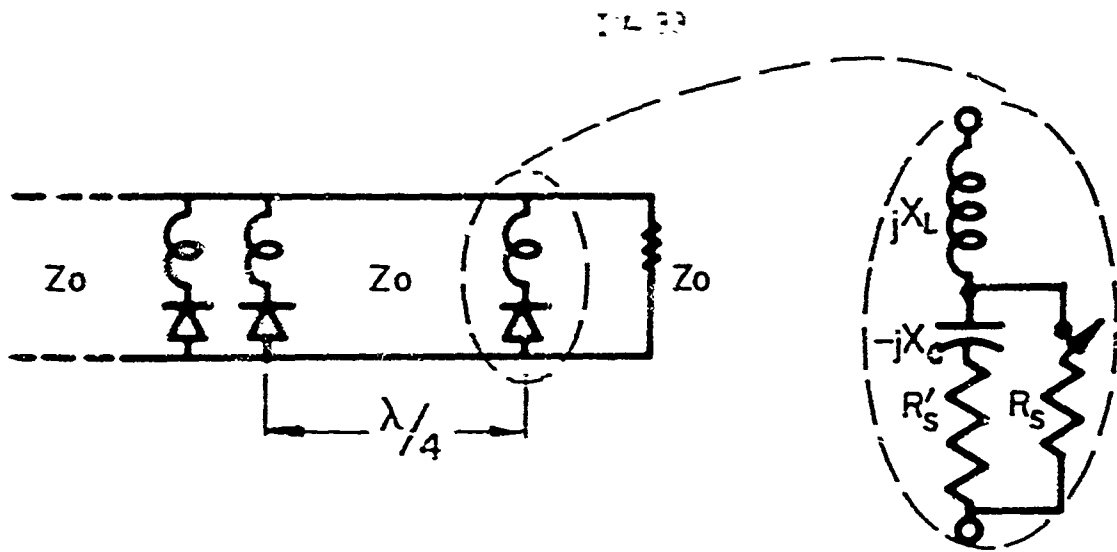


FIGURE 42

may be attributed to the circuit losses with diodes removed; and thus, an insertion loss of about 0.1 decibel per diode pair resulted. This suggests that the unloaded Q of each LC line loading element was approximately 20 and each diode dissipates about 1% of the power transmitted along the line.

Thus, a 1 kilowatt continuous RF power level would be estimated sustainable by this S-band phase shifter model, allowing that each diode could dissipate 10 watts continuously. This is the same continuous power rating expected of the L-band model. The anomaly of equal continuous power handling capability achieved by L and S-band models resulted from the practical fact that the L-band phase shifter did not have equal loss under forward and reverse bias. If characteristic impedance levels of main line and stubs had been chosen to effect equal loss for both bias states of the L-band model, even higher continuous power levels could be sustained.

The unloaded Q value of 20 represented by the S-band switched susceptance elements implies that the diode resistance values, R_F and R_R , were approximately equal at 3000 Mc and had a value of about 1.5 ohms. They were similar to the diodes used in the L-band model for which unequal resistances are measured at L-band for forward and reverse bias. The loss mechanisms of the diode are indicated by this measurement to be such as to cause the effective forward bias resistance to increase and the reverse resistance to decrease with frequency, causing them to be near equal at S-band.

Such behaviour might be explained by noting that skin effect causes the forward biased resistance to increase while the increasing shunt susceptance of the package capacity improves the Q of the reversed biased diode and decreases the apparent series resistance of the simplified model shown in Figure (42). Also, the series RC representation for the reversed biased diode junction, itself, is an approximation which represents the combined diode package contact losses and losses in the Intrinsic region; the former increases with frequency and the latter decreases with frequency.

Since the diode resistance measurements are somewhat difficult to make due to the relatively high Q of the PIN diode at microwave frequencies, these phase shift or insertion loss measurements provide a useful approximate measurement of the absolute value of the diode resistances for forward and reverse bias at 3000 Mc.

d. Voltage Limited Peak Power Capability: Reference to the equivalent circuit for this LC susceptance implementation used in the S-band phase shifter models, see Figure (34), indicates that if the reactance, jX_L , has a magnitude half that of jX_C , then an RF voltage is impressed across the capacitor, in this case the diode junction, equal to twice the line voltage neglecting resistive losses. This is true no matter what value of characteristic impedance line might be used. However, for a given operating power level, the line voltage varies inversely with the square root of the line impedance and thus, the voltage limited peak power handling capabilities should vary inversely with the

characteristic impedance of the main transmission line.

Experimental verification of this expectation was evidenced. In the two-section, four diode, 3.25 ohm model previously described, diodes having voltage breakdown values of about 900 volts were used. These, when reverse biased at -100 volts, were estimated to sustain a maximum applied RF voltage of 560 volts rms. Thus, the line voltage allowably could reach 280 volts rms in the 3.25 ohm section and a burnout peak power capability for the two-section phase shifter then would be estimated at 24 kilowatts. This is considerably lower than the 37 kilowatt measured failure point and the discrepancy may have resulted because the package capacity and junction capacity values were lumped together in the equivalent circuit model. The package capacity, of the order of 0.3 picofarads, carries an appreciable fraction of the current in the susceptance branch and the resulting voltage build-up across the junction capacitor is accordingly less than that which would result were all current to take the path through the junction reactance, jX_C .

The variation of peak power capability, however, was verified in that the 6.25 ohm phase shifter model using similar diodes sustained approximately half the power of the 3.25 ohm model. The sixteen section phase shifter was tested to a burnout of peak power of 16 kilowatts. Failure mechanisms in both models was manifest as a permanent degradation of the voltage breakdown characteristic of the diodes after the high power had been applied under the reverse-bias conditions.

characteristic impedance of the main transmission line.

Experimental verification of this expectation was evidenced. In the two-section, four diode, 3.25 ohm model previously described, diodes having voltage breakdown values of about 900 volts were used. These, when reverse biased at -100 volts, were estimated to sustain a maximum applied RF voltage of 560 volts rms. Thus, the line voltage allowably could reach 280 volts rms in the 3.25 ohm section and a burnout peak power capability for the two-section phase shifter then would be estimated at 24 kilowatts. This is considerably lower than the 37 kilowatt measured failure point and the discrepancy may have resulted because the package capacity and junction capacity values were lumped together in the equivalent circuit model. The package capacity, of the order of 0.3 picofarads, carries an appreciable fraction of the current in the susceptance branch and the resulting voltage build-up across the junction capacitor is accordingly less than that which would result were all current to take the path through the junction reactance, jX_C .

The variation of peak power capability, however, was verified in that the 6.25 ohm phase shifter model using similar diodes sustained approximately half the power of the 3.25 ohm model. The sixteen section phase shifter was tested to a burnout of peak power of 16 kilowatts. Failure mechanisms in both models was manifest as a permanent degradation of the voltage breakdown characteristic of the diodes after the high power had been applied under the reverse-bias conditions.

V CONCLUSIONS

Microwave phase control circuit modes examined may be divided conveniently into two classes. The first considered utilizes the directive properties of a circulator or hybrid coupler to effect matched transmission from a network of controlled reflection coefficient. This may be considered the transmission reflection mode. A second basic circuit effects phase control by periodically spaced, variable reactance elements along the transmission line. Spacings can be chosen to permit matched transmission over a broad bandwidth.

The transmission reflection mode is particularly useful for implementing a continuously variable phase shifter. This was accomplished using terminating networks of a hybrid coupler which contained varactor diodes. Their variable capacity with reverse bias permitted realization of 0° to 180° phase shifters at L and S-bands which were found to have a defined Figure of Merit, F, given approximately by

$$F = \left(\frac{4 \text{ degrees}}{\text{decibel of loss}} \right) \cdot \left(\frac{\text{Diode cut-off Frequency}}{\text{Operating Frequency}} \right)$$

Power level of linear operation was limited to about 1 watt due to the varactor diode's rapid capacity change with applied voltage.

The discrete increment or step phase shifter using PIN diodes did not manifest nonlinear microwave characteristics even at levels exceeding 100 kilowatts with tens of amperes and hundreds of volts applied within a pulse. Transmission reflection phase shifter circuits which used hybrid terminating networks which were essentially switched delay lines were constructed. RF peak power levels of 2.5 to 48 kilowatts

were sustained with phase shift values of 180° and 21.5° respectively.

In general, peak power capability is inversely proportional to the square of the phase shift obtained. Insertion loss, in principle, may be reduced along with phase shift provided lesser values of phase shift are obtained but changes in the circuit impedance levels are necessary.

Operation at increasing RF power levels with reduced values of phase shift obtained per diode suggests the hybrid coupler or circulator component may be eliminated giving rise to the transmission phase shifter mode.

Two basic models of this circuit were constructed, one at L-band and one at S-band. The former utilized switchable length stubs along the main transmission path to effect the necessary controlled susceptance line shunting pairs of the prototype circuit. High power operation up to 140 kilowatts was thusly achieved at L-band. Even more importantly for phased array beam steering applications, the insertion loss values were lower than those obtained with the transmission reflection mode models. A 15 kilowatt peak power, 1 kilowatt continuous power (estimated continuous rating) phase shifter which yielded 0° to 180° phase shift in 8 equal steps had only 0.7 decibels maximum loss, and 0.5 decibels average loss.

The second transmission mode model was designed using the inherent reactances of the PIN diode as switchable phase controlling elements and assumed the simple configuration of a low impedance transmission line with shunt mounted diodes iteratively spaced at quarter wavelength intervals. Likewise, this circuit produced desirable characteristics as a

control element for a high power array antenna. A 6.25 ohm line shunted by 16 diodes provided 0° to 180° phase shift at up to 15 kilowatts peak power and 1000 watts (estimated) continuous power with a maximum total insertion loss of only 0.9 decibels.

In short, microwave semiconductor phase control, particularly in the L and S frequency bands readily is feasible both for low power applications such as automatic instrumentation, countermeasures and trimmer requirements in parallel tube chains as well as high power applications in which the phased array antenna is prominent, as an example.

VI BIBLIOGRAPHY

1. S. B. Cohn, P. M. Sherk, J. K. Shimizu and E. M. T. Jones, "Strip Transmission Lines and Components", Feb. 1957, Final Report - Stanford Research Project 1114, Stanford Research Institute, Menlo Park, California.
2. R. H. Hardin, E. J. Downey, J. Munushian, "Electronically-Variable Phase Shifters Utilizing Variable Capacitance Diodes", Proc. I.R.E., May, 1960, pp. 944-945.
3. A. J. Simmons, "Phase Shift by Periodic Loading of Waveguide and Its Application to Broad Band Circular Polarization", I.R.E. Trans MTT, Dec., 1955.
4. K. E. Mortenson, "Transistor Junction Temperature as a Function of Time", Proc. I.R.E., April 1957.
5. H. N. Dawirs and W. G. Swarner, "A Very Fast, Voltage Controlled Microwave Phase Shifter", The Microwave Journal, June 1962.
6. J. F. White, "Semiconductor Microwave Phase Control", NEREM Record, 1963.
7. J. F. White, "A Diode Phase Shifter for Array Antenna", Digest of 1964 International Symposium of IEEE, MTT Group.
8. M. E. Hines, "Fundamental Limitations of Diode Switching" paper to be published in the Proc. IEEE.
9. L. Stark, R. Burns, et al, "Phased Array Study", Hughes Aircraft Company Study Report, Contract Number NObsr-89427.
10. E. J. Wilkinson, L. I. Parad, W. R. Connervey, "An X-Band Electronically Steerable Phased Array", The Microwave Journal, February 1964.
11. Leo Young, "Tables for Cascaded Homogenous Quarter-Wave Transformers", IRE Trans MTT, April 1960.
12. S. B. Cohn, "Optimum Design of Stepped Transmission-Line Transformers", IRE Trans MTT, April 1955.
13. R. E. Collin, "Theory and Design of Wide-band Multisection Quarter-Wave Transformers", Proc. I.R.E., February 1955.

14. J. Riblet, "General Synthesis of Quarter-Wave Impedance Transformers", I.R.E. Trans MTT, January 1957.
15. K. E. Mortenson, "Microwave Semiconductor Control Devices", The Microwave Journal, May 1964.
16. R. V. Garver, E. G. Spencer and M. A. Harper, "Microwave Semiconductor Switching Techniques", I.R.E. Trans. MTT, October 1958.
17. M. R. Barber, "A High Power Protector Using PIN Diodes", Digest of IEEE MTT Symposium 1963.
18. F. Reggia and E. G. Spencer, "A New Technique in Ferrite Phase Shifting for Beam Scanning of Microwave Antennas", Proc. I.R.E., November 1957.

DISTRIBUTION LIST

Contract Number - 87291

No. of Copies

Chief, Bureau of Ships
Washington 25, D. C.

Attn: Code 681A2B

1

Attn: Code 684

1

Attn: Code 335

1

Chief, Bureau of Weapons
Washington 25, D. C.

1

Director, Naval Electronics Laboratory
San Diego 52, California

1

Director, Naval Research Laboratory
Washington 25, D. C.

Attn: Code 5250

1

Commanding General
U. S. Army Signal Research & Development Labs.
Fort Monmouth, New Jersey
Attn: SIGFM/EL-PEE Mr. N. Kipetz

1

Commanding Officer
Diamond Fuse Laboratories
Connecticut Ave. & Van Ness St., N. W.
Washington 25, D. C.
Attn: Code 250

1

Commanding General
Wright Air Development Center
Wright-Patterson Air Force Base, Ohio
Attn: WWDPVE-1 Mr. G. Duree

1

Commanding General
Rome Air Development Center
Griffiss Air Force Base, New York
Attn: Mr. P. Romanelli

1

Commanding General
Air Force Cambridge Research Center
Air Research & Development Command
L. G. Hanscom Field
Bedford, Mass. Mr. C. E. Ellis

1

Advisory Group on Electron Devices
346 Broadway
New York, N. Y.

3

No. of Copies

Armed Services Technical Information Agency
Arlington Hall
Arlington, Virginia

7

Commander (Code 753)
U. S. Naval Ordnance Test Station
China Lake, California
Attn: Technical Library

1

New Mexico State University
Physical Science Laboratory
Box 548
University Park
New Mexico

1